EurJOC
European Journal of Organic Chemistry

Review
doi.org/10.1002/ejoc.202200417

Chemistry Europe
European Chemical Societies Publishing

www.eurjoc.org

VIP *Very Important Paper*

Special Collection

Synthetic Applications of Photocatalyzed Halogen-Radical Mediated Hydrogen Atom Transfer for C–H Bond Functionalization

Stefano Bonciolini,[a] Timothy Noël,[a] and Luca Capaldo*[a]

Luca Capaldo was nominated to be part of this collection by EurJOC Board Member Stefano Protti.

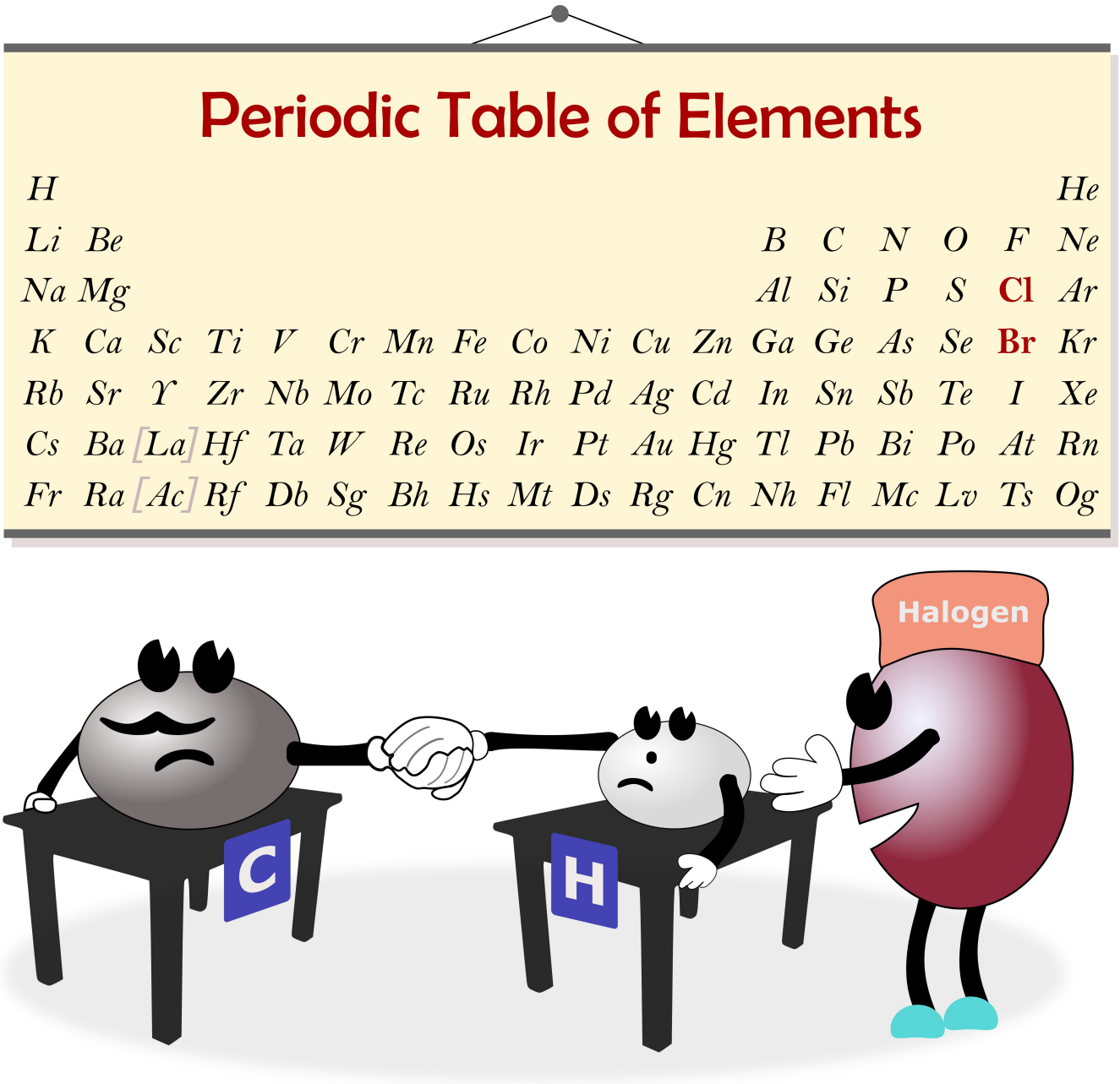

The opportunity to activate C(sp^3)–H bonds via homolytic cleavage by means of halogen radicals has long been disregarded in synthetic endeavors due to the unpredictable selectivity. Nowadays, photocatalysis has established itself as a method of choice for the generation of such reactive intermediates under mild conditions. This Minireview collects recent examples showcasing how photocatalytic manifolds have been used to tame aggressive halogen radicals to activate C(sp^3)–H bonds via Hydrogen Atom Transfer (HAT) for synthetic purposes. In the last section of this work, we address site-selectivity issues posed by this methodology and show how it can be guided through the judicious choice of reaction conditions.

1. Introduction

Hydrogen Atom Transfer (HAT) is the concerted movement of a proton (H^+) and an electron (e^-) between two functional groups in one single kinetic step. Despite its simplicity, a considerable amount of research has been carried out to understand the intricacies of this step[1,2] and outline a general mechanistic framework. In fact, it is a common position that HAT belongs to the more general category of Proton-Coupled Electron Transfer (PCET) processes, where the targeted substrate undergoes a redox event and deprotonation with two different molecular entities (an oxidant and a base, respectively).[3–5]

Besides its importance in environmental and biological processes,[6] HAT has also rapidly emerged as a powerful substrate activation manifold in organic synthesis. This is mainly because synthetic chemists have realized that it conveniently enables the functionalization of C–H bonds, even in complex molecules, without the need to introduce a directing moiety.[7] More importantly, great levels of site-selectivity can be obtained by mastering substrate-dependent effects (torsional, steric, polar, stereoelectronic, (hyper)conjugative effects, etc.) and medium-dependent effects (e.g., hydrogen-atom abstractor, additives, solvent, etc.).[8–12]

However, in order to homolytically break a C–H bond, a considerable amount of energy (typically >90 kcal mol^{-1})[13] is required, which calls for the generation of aggressive intermediates. Traditional HAT involves *p*-block radicals such as, for example, *tert*-butoxyl (*t*-BuO$^\bullet$) or cumyloxyl (CumO$^\bullet$) radicals,[14–16] namely electrophilic O-centered radicals that can be generated via photolysis[17] of the corresponding peroxide or heating a solution containing the hydroperoxide and a catalytic amount of a transition metal (typically copper).[18]

More recently, photocatalysis has emerged as an extremely valuable and versatile tool in organic synthesis because it allows the use of the greenest and cheapest form of energy (i.e. photons) for synthetic purposes.[8,19,28,20–27] This happens thanks to the aid of a species that is purposely added to the reaction mixture, i.e. the photocatalyst (PC), which is responsible for converting light energy into chemical energy for substrate activation. A photocatalyzed version of HAT exists too, and can be classified into two main categories: direct HAT and indirect HAT (Scheme 1).[29]

In the former case, a suitable PC absorbs a photon and, once in the excited state, performs the HAT step. The main requirement for such a PC is to have a "Y=O" (Y: metal or carbon) moiety that turns into a "$^\bullet$Y–O$^\bullet$" one when in the excited state: in a certain sense, the behavior of this electrophilic O-centered radical is reminiscent of that of the *p*-block radicals mentioned above. After hydrogen abstraction, a "$^\bullet$Y–OH" species is generated, and the photocatalytic cycle is eventually closed via re-oxidation of the PC (Scheme 1A). Very recently, several reviews have been written on direct HAT and the reader is kindly referred to them to gain deeper insights into this methodology.[8,30,31] However, one can easily notice that the range of transformations accessible with direct HAT is somehow limited by (i) the requirement for the PC to possess a Y=O moiety to trigger the desired HAT step, (ii) the limited number of photocatalysts known to perform this HAT step in low catalytic loadings (<20 mol%) and (iii) the photophysical and physicochemical properties of the photocatalysts itself (UV-light is typically required, selectivity biased by steric interactions, solubility in the reaction crude, robustness in the presence of additives, etc…). Hence, a more versatile approach is needed to perform more elaborated transformations.

In indirect HAT, the photocatalyst takes care of absorbing light and, once in the excited state, converts a reaction additive

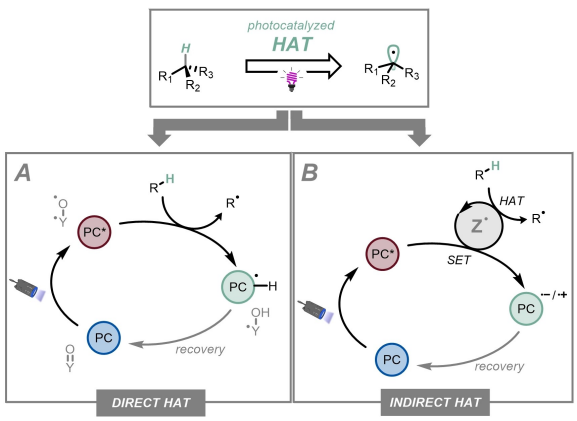

Scheme 1. Photocatalyzed HAT can be classified as direct HAT (A) or indirect HAT (B).

[a] S. Bonciolini, Prof. Dr. T. Noël, Dr. L. Capaldo
Flow Chemistry Group, Van 't Hoff Institute for Molecular Sciences (HIMS)
University of Amsterdam
Science Park 904, 1098 XH, Amsterdam, The Netherlands
E-mail: l.capaldo@uva.nl
www.NoelResearchGroup.com

Part of the "NextGenOrgChem" Special Collection.

into the active H-atom abstractor (Z•), either via single electron transfer (SET) or Energy Transfer (EnT) (Scheme 1B). At the expense of adding an extra reagent in the reaction mixture, this manifold allows to separate the role of light-absorbing species (PC) and that of H-atom abstracting one (Z•). The main advantage of this (perhaps) subtle conceptual difference is that most common visible-light absorbing photoredox catalysts can be standardly used, while the HAT step can be tuned by varying the additive from which Z• is generated. Several additives have been proposed in the literature to generate different abstracting species: O-, N-, S-, B- and halogen-centered radicals.[29,30,32,33]

Recently, the latter ones are attracting a great deal of attention from the scientific community and this is mainly for two reasons: (i) halogen atoms are aggressive, electrophilic radicals (e.g., BDE for HCl is 103 kcal mol^{-1}),[34] thus thermodynamically accessing a wide portfolio of C–H bonds and (ii) the only waste generated upon this indirect HAT step is a strong acid (HX), which can be conveniently neutralized upon workup or by directly adding a base in the reaction mixture.

Table 1 gathers data that are useful for discussion throughout this review, namely redox potentials of the X•/X$^-$ couples and BDEs (Bond Dissociation Energies) of the H–X bonds (X: halogen). A short description of the categories of C–H bonds that can be cleaved by the halogen is also given. Thus, while bromide is easier to oxidize than chloride, suggesting that milder conditions can be used to trigger the desired HAT step, the resulting bromine radical is a weaker H-abstractor than the chlorine radical. This combination endows the former with a wider functional-group tolerance; however, the latter is needed to activate more recalcitrant aliphatic C–H bonds. This augmented reactivity of chlorine, however, comes at the expenses of the selectivity in the HAT step. It is worth mentioning that the oxidation of iodide to the corresponding iodine radical is an even more favorable process, but the low BDE of the H–I bond makes it unsuitable for HAT.

Table 1. Relevant data for halogen radical-mediated HAT.

Halide	E^0 [X•/X$^-$][a] [V]	BDE H–X (kcal mol^{-1})	Applications
Cl$^-$	+2.03 V[35]	103[34]	(un)activated aliphatic C(sp^3)–H bonds
Br$^-$	+1.60 V[35]	88[36]	C(sp^3)–H bonds (tertiary, benzylic, α-oxo, α-amino) and formyl C(sp^2)–H (aldehydes)
I$^-$	+1.06 V[35]	71[36]	Not useful for HAT

[a] Potential vs Saturated Calomel Electrode (SCE).

In this Minireview, we aim to gather examples in the recent literature regarding the photocatalytic generation of halogen atoms for indirect HAT for C–H bond activation. In doing so, we mainly focused on the preparative aspects of this chemistry. Similarly, we excluded those reports where the formation of the halogen atom does not depend on a photocatalyst, but is a consequence of photoinitiated and photochemical events.[37–41] Finally, we did not consider those cases where one of the substrates also works as the photocatalyst,[42] as these should be more properly referred to as photochemical approaches. It is worth mentioning that halogen radical-mediated HAT has been

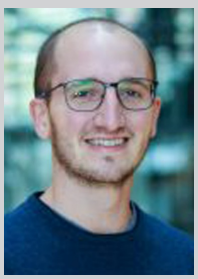

Stefano Bonciolini was born in 1994 in San Miniato (Tuscany, Italy) and received his M.Sc. (cum laude) in Organic Chemistry at the University of Pisa in 2019. During his M.Sc., he worked on asymmetric α-amination reactions promoted by chiral organocatalysts of 3-substituted 2-oxindole compounds under the supervision of Prof. Alessandro Mandoli. Later on, he joined Prof. Marcus Baumann group at the UCD (Dublin, Ireland) as an Erasmus student for 5 months where he carried out research on photocatalytic HAT transformations in continuous flow. From February 2021 he is a Ph.D. candidate at the University of Amsterdam (advisor: Prof. Timothy Noël) in the frame of the Marie S. Curie ITN network PhotoReAct on photochemical transformations in microflow reactors.

Timothy Noël currently holds a position as Full Professor at the University of Amsterdam, where he is the chair of Flow Chemistry. His research interest ranges from organic chemistry to chemical engineering and encompass more specifically flow chemistry, organic synthesis and synthetic catalytic methodology development. His work received several awards, including the DECHEMA prize (2017), the Hoogewerff Jongerenprijs (2019), the IUPAC-ThalesNano prize in flow chemistry and microfluidics (2020) and the KNCV Gold Medal (2021). He also serves as editor-in-chief of Journal of Flow Chemistry.

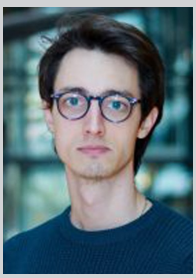

Luca Capaldo was born in Milan, Italy in 1991. After an Erasmus Traineeship in the De Cola group at the Institut de science et d'ingénierie supramoléculaires and a visiting period as a Ph.D. student in the Yoon Group at the University of Wisconsin–Madison, he received his doctorate in Chemical and Pharmaceutical Sciences at the University of Pavia in 2019 (advisor: Prof. M. Fagnoni). After a 2-years postdoctoral fellowship in Pavia (PI: Prof. D. Ravelli), Luca joined the Flow Chemistry Group at the University of Amsterdam as a Marie Curie Fellow (advisor: Prof. T. Noël) to develop novel synthetic methodologies based on photocatalyzed HAT in flow.

also used to activate O–H bonds in alcohols and carboxylic acids.[43,44]

Given the above, the covered examples can be classified into three categories depending on the operating mechanism: photolysis triggered by Ligand-to-Metal Charge Transfer (LMCT), photoredox catalyzed outer-sphere single-electron transfer and energy transfer (Scheme 2).

As for the former, the generation of halogen atoms via photolysis of a M–X bond is typically a consequence of an inner-sphere electron transfer (namely, a LMCT event) within a complex.[45] In detail, the absorption of a photon of a suited energy promotes a charge transfer from the ligand (e.g. chloride or bromide) to the metal via an inner-sphere electron transfer: the net result is the production of the halogen atom and a mono-electronically reduced metal center. This process is mostly known for nickel, iron, copper, cerium and titanium halide complexes (Scheme 2A).

Another possibility is the generation of halogen atoms via photoredox catalysis, which relies on the use of photocatalysts whose reduction potential in the excited state is high enough to oxidize halides via an outer sphere electron transfer (see Table 1 and Scheme 2B).

Finally, halogen atoms can also be generated via energy transfer, where the photocatalyst (mostly iridium-based complexes) absorbs a photon and ceases energy to a nickel complex, thus promoting the homolytic cleavage of a Ni–X bond formed during the reaction. It is important to remark here that a Ni^{III} species is not involved in this last scenario (Scheme 2C).

As one of the major concerns related to the use of halogen-mediated Hydrogen Atom Transfer is often site-selectivity for synthetic applications, we deemed appropriate to devote the last section of this work to showcase how this can be tweaked upon a judicious choice of reaction conditions.

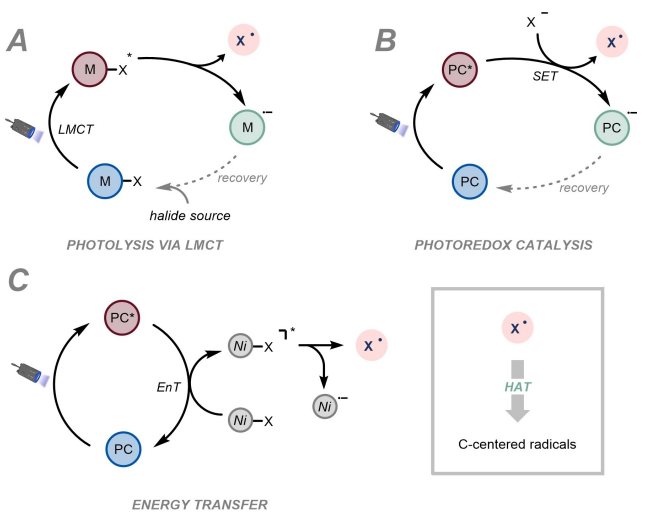

Scheme 2. Three strategies have been devised for the photocatalytic generation of halogen radicals: A) LMCT-triggered photolysis, B) photoredox catalysis and C) energy transfer.

2. Generation of Halogen Radicals via LMCT-Triggered Photolysis

The ability of M–X bonds to undergo light-triggered homolysis has been known since 1962, when Kochi reported the photolysis of $CuCl_2$ to generate chlorine atoms.[46] Prompted by a colleague's (Dr. W. S. Anderson) observation that Cu^{I} salts were formed upon exposure of a mixture of $CuCl_2$ and butadiene to sunlight, he decided to qualitatively investigate the photochemical reactivity of this salt with ethers, alcohols and unsaturated hydrocarbons. Based on product distribution, he concluded that the irradiation with UV-light by means of a mercury lamp under inert atmosphere generated chlorine atoms together with reduced Cu^{I} species.

Later on, Shul'pin observed a similar behavior with $FeCl_3$: irradiation of this salt with a luminescent street lamp in the presence of hydrocarbons in air-equilibrated conditions led to the formation of oxygenated products.[47,48] The authors ascribed the result to a photoinduced electron transfer between the substrate and the excited state of $FeCl_3$, followed by "proton detachment" to afford the C-centered radical. Finally, reaction with molecular oxygen afforded the corresponding end products. A similar investigation was conducted by Takaki where it was found that also $CuCl_2$ showed a similar behavior, even when using sunlight.[49,50]

After these seminal examples, several other works reporting halogen photoelimination started to appear; however, these were mainly focused on the application of this process as an energy-harvesting strategy.[51,52] Contrarily, synthetic applications did not emerge until after 2015, when Nocera reported two works showing the peculiar behavior of a suite of nickel complexes.[53,54] In detail, he found that irradiation of Ni^{III}–Cl (and Ni^{III}–Br) species, generated in situ upon oxidation by $PhICl_2$, undergo prompt Ni–X homolysis as a consequence of a Ligand-to-Metal Charge Transfer (LMCT) efficiently triggered at 370 or 434 nm. Even though photoproducts were not characterized, photogenerated halogen atoms were expected to react via HAT with the solvent (e.g. CH_3CN).

The abovementioned examples shook the synthetic community that, in fact, started using this activation manifold to invent more and more sophisticated chemical transformations via indirect HAT. The examples reported have been classified below according to the metal involved in the LMCT.

2.1. Nickel

Capitalizing on Nocera's preliminary findings, the Doyle group reported a series of $C(sp^3)$–$C(sp^2)$ cross-coupling reactions between hydrogen-atom donors and aryl/acyl chlorides via HAT.[55] For example, in 2016, they found that when a tetrahydrofuran solution of **3.1** was irradiated with a blue LED lamp in the presence of an Ir-based photocatalyst, $Ni(cod)_2$ and 4,4′-di-tert-butyl-2,2′-bipyridine (**3.3**) as the ligand, the expected cross-coupled product **3.2** was obtained in 70% yield after isolation (Scheme 3A).[56] As for the mechanism, Ni^0 undergoes

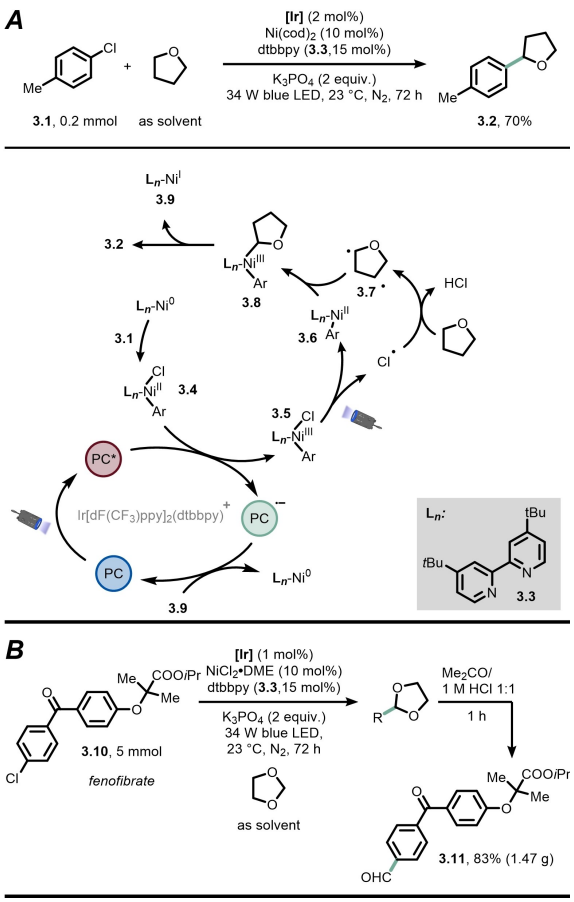

Scheme 3. A) Arylation of ethers enabled by the catalytic generation of chlorine radicals via LMCT-triggered homolysis of a Ni^{III}–Cl bond; B) Formylation of aryl chlorides through the photocatalytic generation of chlorine radicals via LMCT-triggered homolysis of a Ni^{III}–Cl bond.

oxidative addition onto **3.1** to form the corresponding Ar–Ni^{II}–Cl species (**3.4**). Next, the excited state of the photocatalyst oxidizes **3.4** to afford a Ni^{III} species (**3.5**), which rapidly undergoes photolysis via LMCT to deliver the desired chlorine atom (Cl•) and **3.6**. Tetrahydrofuran is activated by the latter intermediate to afford HCl and an α-oxyalkyl radical (**3.7•**), which is intercepted again by the Ni^{II} center to give complex **3.8**. Eventually, reductive elimination affords product **3.2** and the exhausted photocatalyst is re-oxidized by the obtained Ni^{I} species (**3.9**).

When 1,3-dioxolane was used as the hydrogen-atom donor (Scheme 3B), the formylation of aryl chlorides was achieved.[57] Thus, the 2-position of 1,3-dioxolane (used as solvent) was activated by the chlorine radical and 2-arylated dioxolanes were obtained. The product was not isolated, but hydrolyzed instead to give the corresponding aryl aldehyde. It is interesting to note that, while in the previous example an unstable Ni^0 complex was necessary, the use of a bench-stable $NiCl_2 \cdot DME$ (DME: 1,2-dimethoxyethane) was tolerated in this case, which enabled scale-up for the functionalization of fenofibrate (**3.10**): ca. 1.5 g of the corresponding formylated product **3.11** was obtained (83%).

Later on, the same group used LMCT-triggered homolysis of a Ni^{III}–Cl bond to achieve also the methylation of (hetero)aryl chlorides (Scheme 4).[58] Thus, the irradiation of an orthoformate solution of aryl chlorides **4.1** under otherwise identical conditions led to the formation of product **4.2** in 58% yield after isolation.

Herein, Cl• performs HAT onto the tertiary position of orthoformate to give **4.3•**, which undergoes fragmentation to ultimately yield a methyl radical (**4.4•**). The methyl radical is recaptured by the nickel catalytic cycle and product **4.2** is obtained after reductive elimination. This methodology was also extended to biologically relevant aryl chlorides such as a zomepirac derivative (**4.5**, a NSAID), fenofibrate (**4.6**, used to treat abnormal blood lipid levels) and loratidine (**4.7**, used to treat allergies). Remarkably, the procedure was amenable to other chloride-containing electrophiles such as aromatic and aliphatic acyl chlorides, thus enabling the synthesis of methyl ketones.

The same group also achieved the esterification of unactivated C(sp^3)–H bonds (Scheme 5A) by replacing aryl chlorides with chloroformates.[59] The same transformation could be extended to benzylic and α-to-N and α-to-O C(sp^3)–H bonds by increasing the temperature to 40 °C. The mechanism is similar to that reported in Scheme 3A: Ni^0 undergoes oxidative addition to a chloroformate derivative (**5.1**) to generate the corresponding Cl–Ni^{II}–COOR species. Halogen photoelimination, followed by HAT from cyclohexane, radical capture and reductive elimination delivered ester **5.2** in 60% yield. The authors also noticed partial decomposition of **5.1** due to the basic conditions adopted (K_3PO_4, 2 equiv.) to form **5.3** as a by-product.

In another instance, the Hong group reported the acylation of hydrocarbons via indirect HAT mediated by chlorine atom

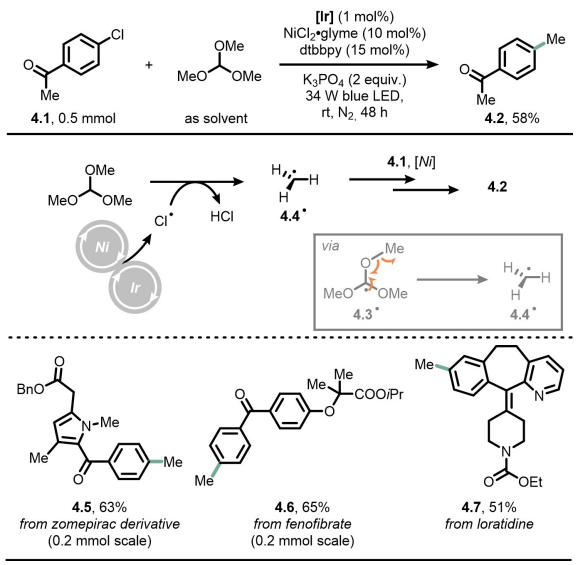

Scheme 4. Methylation of (hetero)aryl chlorides enabled by the catalytic generation of chlorine radicals via LMCT-triggered homolysis of a Ni^{III}–Cl bond. The methyl radical is generated via the fragmentation of the tertiary radical of **4.4•**.

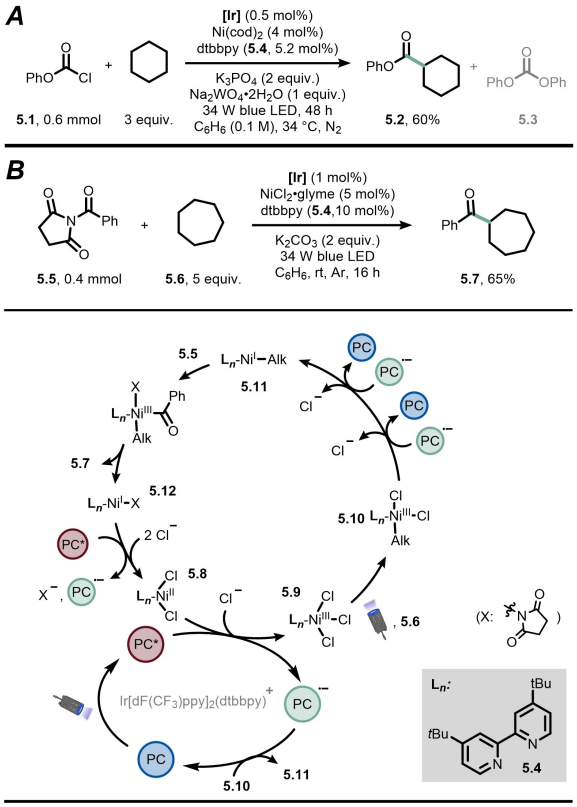

Scheme 5. A) Esterification of unactivated C(sp^3)–H bonds through the photocatalytic generation of chlorine radicals via LMCT-triggered homolysis of a Ni^{III}–Cl bond. B) Acylation of hydrocarbons enabled by the catalytic generation of chlorine radicals via LMCT-triggered homolysis of a Ni^{III}–Cl bond.

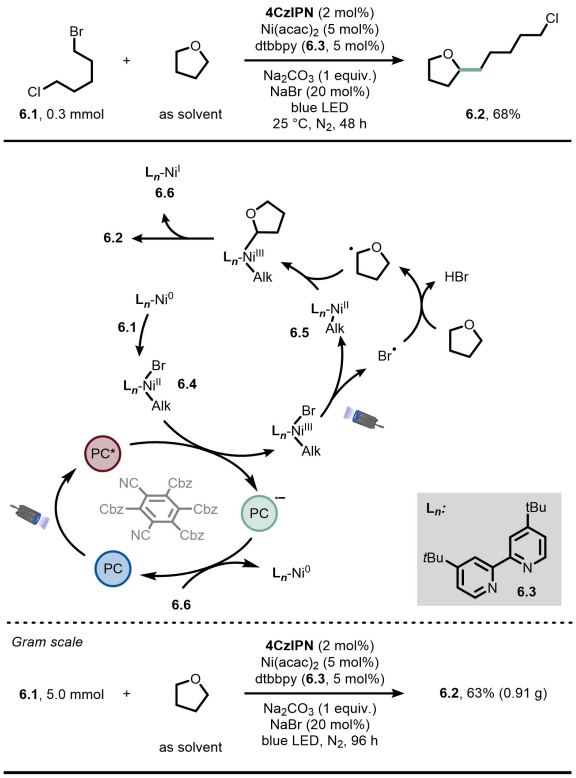

Scheme 6. C(sp^3)–C(sp^3) cross-coupling of alkyl bromides and ethers enabled by the catalytic generation of bromine radicals via LMCT-triggered homolysis of a Ni^{III}–Br. 4CzIPN: 1,2,3,5-Tetrakis(carbazol-9-yl)-4,6-dicyanobenzene, 2,4,5,6-Tetrakis(9H-carbazol-9-yl) isophthalonitrile.

(Scheme 5B).[60] In detail, when **5.5** (0.4 mmol) and cycloheptane (**5.6**, 5 equiv.) were irradiated with a blue LED in the presence of an Ir-based photocatalyst, $NiCl_2 \cdot$glyme (5 mol%) and **5.4** (10 mol%), ketone **5.7** was obtained in 65% yield. Thanks to a detailed DFT-driven mechanistic analysis, the authors disclosed a scenario that begins with the reductive quenching of the excited state of the photocatalyst by the Ni^{II} species **5.8**. The resulting Ni^{III} complex (**5.9**) rapidly captures a chloride anion. Upon photolysis of the Ni–Cl bond, HAT from **5.6** and radical rebound, the organonickel compound **5.10** is formed: the authors proposed an inner sphere σ-bond metathesis for the formation of the latter complex. Next, double reduction by the spent photocatalyst Ir^{II} affords a Ni^{I} species (**5.11**) that can undergo oxidative addition onto **5.5** and then reductive elimination to give **5.7**. Finally, a photoinduced SET from the resulting Ni^{I} species **5.12** to the photocatalyst closes the nickel catalytic cycle. Remarkably, the oxidative addition, and not the hydrogen atom transfer, was proposed as the rate-determining step in this case.

Quite recently, König and co-workers designed a chlorine-radical-mediated process for the C(sp^3)–C(sp^3) cross-coupling of alkyl bromides and ethers (Scheme 6).[61] When a tetrahydrofuran solution of alkyl bromide **6.1** was irradiated with blue light in the presence of 4CzIPN as the photocatalyst and $Ni(acac)_2$, product **6.2** was obtained in 68% yield. Interestingly, the functionalization occurred chemoselectively and the chlorine atom was preserved. As for the mechanism, an in-situ generated Ni^0 species (by double photocatalytic reduction) undergoes oxidative addition onto **6.1** to form Alk–Ni^{II}–Br species **6.4**. Oxidation of the latter by the excited state of the photocatalyst affords a Ni^{III} species, which is photolyzed to deliver complex **6.5** and a bromine radical, in turn responsible for the activation of tetrahydrofuran via HAT. The so-formed C-centered radical is trapped by **6.5** and **6.2** is formed upon subsequent reductive elimination.

Finally, the photocatalytic cycle is closed by reduction of the Ni^{I} species **6.6** back to Ni^0. It is important to mention that when the bromine atom on **6.1** was replaced with triflate or iodine, the reaction did not proceed, thus providing evidence for the importance of the bromine atom in the mechanism. The methodology proved to be robust, allowing the conversion of **6.1** to **6.2** in 63% yield on a gram scale after 96 hours of irradiation.

Wu and co-workers adopted indirect HAT by chlorine atom to achieve the hydroalkylation of internal alkynes (Scheme 7).[62] In particular, when a tetrahydrofuran solution of alkyne **7.1** was irradiated with blue light in the presence of an Ir-based photocatalyst, $NiCl_2$ and 4,4′-di-tert-butyl-2,2′-bipyridine (**7.3**, dtbbpy) as the ligand, regioisomers **7.2** and **7.2′** were obtained in 72% overall yield (5:1 ratio) with an excellent *E*-selectivity.

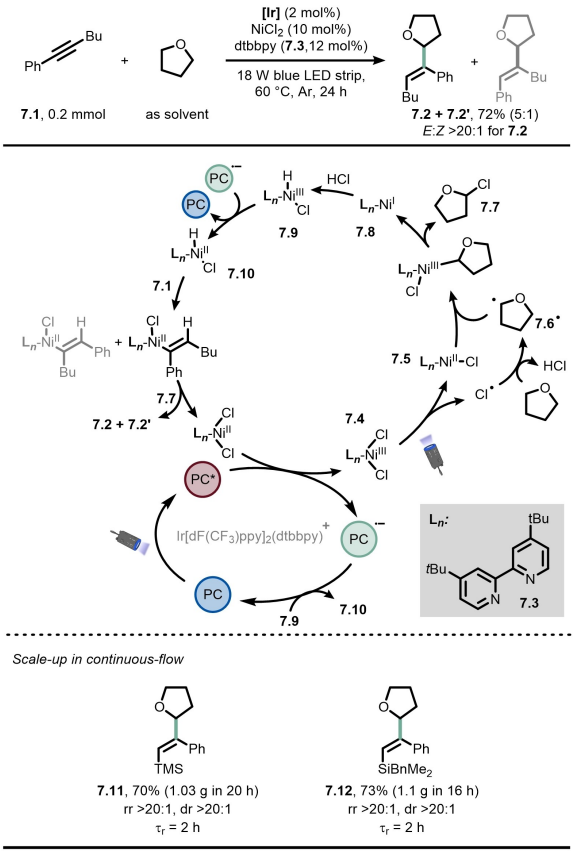

Scheme 7. Hydroalkylation of internal alkynes enabled by the catalytic generation of chlorine radicals via LMCT-triggered homolysis of a Ni^{III}–Cl bond.

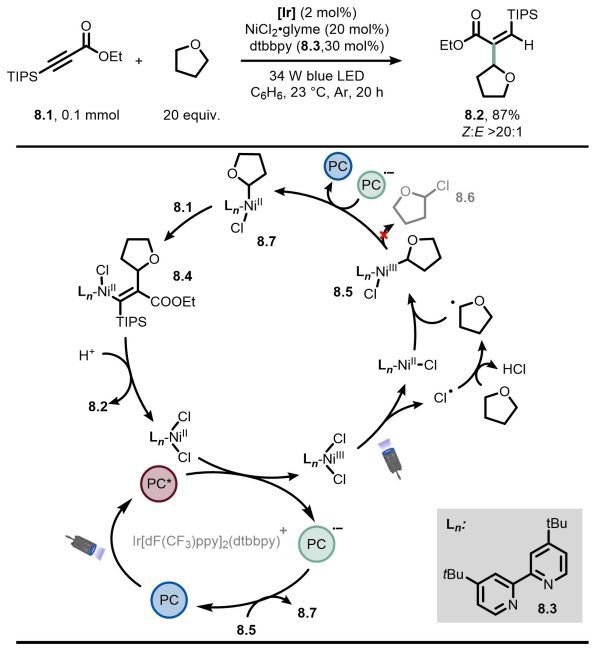

Scheme 8. Hydroalkylation of ynones, ynoates, and ynamides enabled by the catalytic generation of chlorine radicals via LMCT-triggered homolysis of a Ni^{III}–Cl bond.

Intrigued by the unusual regioselectivity for radical addition onto alkynes and by the lack of reactivity when using $Ni(cod)_2$ instead of $NiCl_2$, the authors undertook a meticulous mechanistic investigation. Thus, Ni^{II} reductively quenches the excited state of the photocatalyst to give the photoactive Ni^{III} species (**7.4**), from which Cl• is generated upon light absorption. HAT from tetrahydrofuran (used as solvent) affords intermediate **7.6•** that rebounds to **7.5** and, after reductive elimination, 2-chlorotetrahydrofuran (**7.7**) and a Ni^{I} species (**7.8**) are formed. Protonation of the latter leads to the formation of the nickel-hydride species **7.9**, which is reduced by the exhausted state of the photocatalyst to a Ni^{II} species (**7.10**).

Subsequent hydronickelation of **7.1** results in the formation of vinyl nickel intermediate: regioselectivity arises from this step. Finally, nucleophilic substitution onto **7.7** affords product **7.2** (and **7.2'** as a minor regioisomer). The reaction could be performed efficiently on a gram scale by adopting a continuous-flow technology;[63,64] thus, **7.11** and **7.12** were both formed in ca. 70% yield with good regio- and diasteroselectivity.

One year later, the Hong group adopted a similar approach for the hydroalkylation of ynones, ynoates and ynamides (Scheme 8).[65] For example, when a benzene solution of ynoate **8.1** and tetrahydrofuran was irradiated in the presence of an Ir-based photocatalyst, $NiCl_2$ and dtbbpy, the α-alkylated product **8.2** was obtained in 87% yield (*Z*:*E* > 20:1) after isolation. Interestingly, in order to explain the observed regio- and stereochemistry, the authors invoked a different mechanistic scenario respect to the one reported by Wu, proposing that the Ni^{III} species **8.5** undergoes reduction by the spent PC and migratory insertion[66] with ynone **8.1** rather than reductive elimination to give 2-chlorotetrahydrofuran (**8.6**). In this way, a vinyl Ni complex (**8.4**) is generated and product **8.2** is delivered upon protodenickelation.

2.2. Iron

Iron has been used as a metal center to promote the generation of chlorine radicals for indirect HAT; however, unlike nickel, it does not require dual catalytic conditions. In other words, while in the case of nickel a photoredox catalyst is required to form the photolabile Ni^{III}–Cl species, Fe^{III}–Cl species are bench-stable, but can directly produce halogen atoms upon irradiation.

For example, the Duan group reported the use of iron to generate Cl• via a LMCT process triggered by UV-light irradiation. Thus, in one case, they reported the functionalization of light alkanes and other compounds via a radical hydroalkylation (Scheme 9A).[67]

For example, ethane, propane and butane were readily activated by $FeCl_3 \cdot 6H_2O$ (1-3 mol%) under irradiation at 365 nm. In the case of butane (**9.1**), the C-centered radical generated via HAT was trapped by compound **9.2** to give product **9.3** in excellent yield (92%) even if with a low regioisomeric ratio (2.1:1). Besides light alkanes, also liquid alkanes, ethers, ketones and alkyl aromatics could be function-

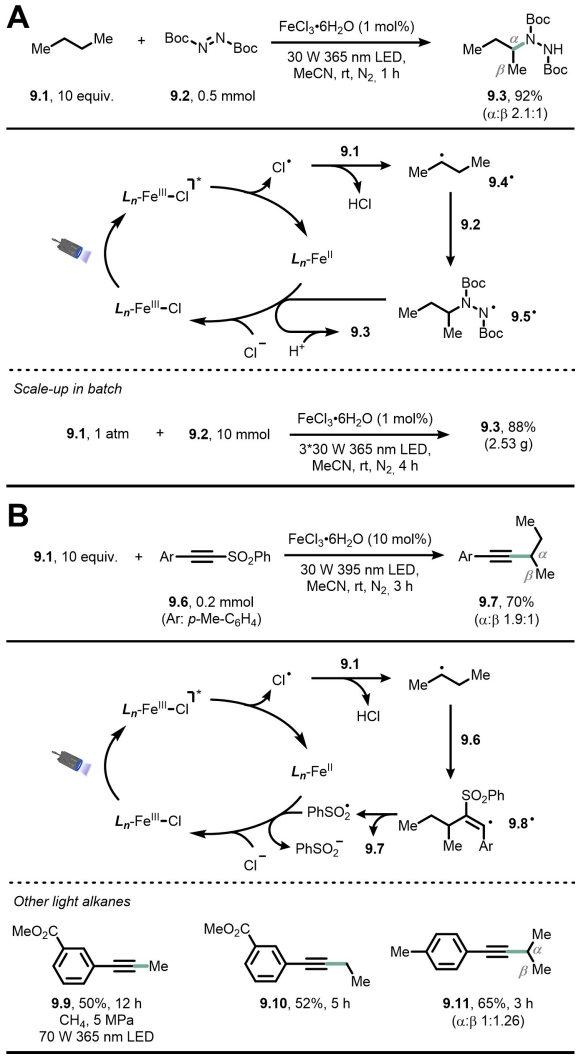

Scheme 9. A) Amination of light alkanes enabled by the catalytic generation of chlorine radicals via LMCT-triggered homolysis of a Fe^{III}–Cl bond. B) SOMOphilic alkynylation of alkanes enabled by the catalytic generation of chlorine radicals via LMCT-triggered homolysis of a Fe^{III}–Cl bond.

alized, and the reaction performed good when replacing **9.2** with electron-poor olefins as well. As for the mechanism, a LMCT triggers the homolysis of a Fe^{III}–Cl bond to form Cl•, in turn accountable for the HAT step from the alkane to give intermediate **9.4•**.

The latter intermediate is trapped by **9.2**, and the resulting electrophilic radical **9.5•** is responsible for closing the photocatalytic cycle and delivering the product. Remarkably, the reaction between **9.1** and **9.2** performed equally well on a 10 mmol scale in batch, delivering ca. 2.5 g of the expected product, corresponding to a 88% yield.

In a very recent follow-up work the authors studied in detail the LMCT process via DFT calculations and also provided evidence for the absence of a radical-chain mechanism.[68]

Under similar conditions, the SOMOphilic alkynylation of light alkanes was also achieved (Scheme 9B).[69] Thus, when **9.1** was reacted with alkynyl sulfone **9.6** in the presence of $FeCl_3 \cdot 6H_2O$ (10 mol%), alkyne **9.7** was obtained in good yield (70%, rr ~2:1). From a mechanistic standpoint, UV-light absorption triggers a LMCT to form the chlorine radical, which activates butane via HAT. Next, the resulting C-centered radical is trapped by **9.6** to give vinyl radical **9.8•**. Finally, product **9.7** is obtained upon the loss of $PhSO_2$•, which is also accountable for the closure of the photocatalytic cycle. Good yields were also obtained in the case of alkynylation of methane (**9.9**), ethane (**9.10**) and propane (**9.11**). The latter showed an unusual regioselectivity, the primary position being functionalized preferentially (1°:2° 1.26:1). This result was justified as a consequence of a delicate interplay between statistical factors, stability of the resulting C-centered radicals and steric factors.

In the same year, Rovis and co-workers reported the use of iron chloride to promote the Dowd–Beckwith rearrangement via HAT (Scheme 10).[70] Thus, when a CH_3CN solution of pinacolone (**10.1**) and acrylate **10.2** (0.3 mmol, 0.3 M) was irradiated with UV-light (390 nm) in the presence of a catalytic amount of $FeCl_3$ (25 mol%), a mixture of products **10.3** and **10.4** was obtained in a ratio of 1:1.4 (59% total yield). When the same reaction mixture was irradiated at a higher temperature (60 °C) and lower concentration (0.1 M), the intramolecular radical rearrangement was favored (**10.3:10.4** 1:10, 64% total yield). In detail, the mechanism proposed by the authors starts with the formation of a tetrachloro ferrate anion, which readily undergoes photolysis to generate the chlorine radical, in turn responsible for HAT on **10.1**.

The thus-generated primary radical **10.5•** can either be directly trapped by **10.2** to afford product **10.3** via a traditional Giese reaction pathway or undergo the Dowd–Beckwith rearrangement. Thus, **10.5•** can cyclize to give oxyl radical **10.6•**, which is prone to β-scission to give radical **10.7•**. From here, radical addition onto **10.2** delivers product **10.4**. The authors concluded that higher temperatures and lower concentration promote the latter reaction pathway.

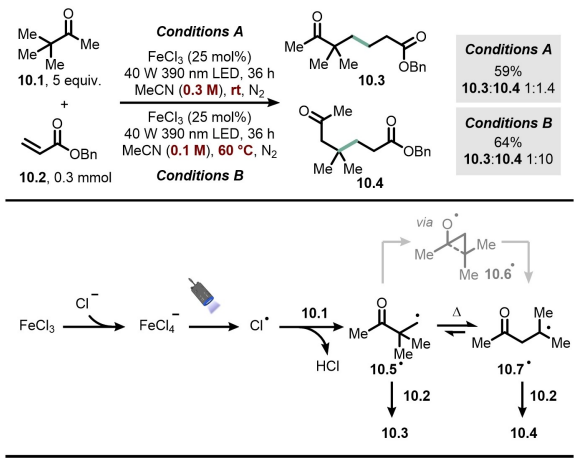

Scheme 10. Radical hydroalkylation via Dowd–Beckwith rearrangement enabled by the catalytic generation of chlorine radicals via LMCT-triggered homolysis of a Fe^{III}–Cl bond.

Later on, the authors reported an extension of this methodology for the alkylation of nonactivated C(sp^3)–H bonds distal to electron-withdrawing moieties via Giese addition.[71]

In another instance, the Hu group reported the generation of Cl• to promote the C–C bond cleavage via β-scission of an oxyl radical.[44] In this case, Cl• is used to cleave an O–H bond to afford the O-centered radical that undergoes β-scission.

2.3. Copper

The synthetic use of copper to promote the formation of halogen atoms for HAT has been seldom reported. As already mentioned above, preliminary studies date back to the seminal studies by Kochi in the 60s, followed by Takaki's reports published almost 20 years ago, but synthetic endeavors have appeared only recently.

For example, the radical hydroalkylation of electron-poor olefins (Giese reaction) has been reported (Scheme 11).[72] In detail, when an acetonitrile solution of cyclohexane (**11.1**, 5 equiv.) and acrylate **11.2** (0.3 mmol) was irradiated under UV-light (390 nm) in the presence of $CuCl_2$ and an extra source of chloride anions (LiCl, 50 mol%), product **11.3** was obtained in excellent yields (92%). As for the mechanism, the authors proposed that a trichlorocuprate anion is formed in situ in the presence of LiCl and undergoes a LMCT process when irradiated with the proper wavelength. Photolysis of the Cu^{II}–Cl bond affords the desired chlorine atom that, in turn, activates **11.1** via HAT to give the expected C-centered radical. The latter intermediate is trapped by **11.2** to give radical adduct **11.4•**, which is intercepted again by the copper center and, after protodecupration, product **11.3** is formed concomitantly with the closure of the photocatalytic cycle.

2.4. Cerium

Following to Kochi's preliminary results,[73] the Zuo group has recently capitalized on cerium photocatalysis for the direct generation of alkoxy radicals from free alcohols via an LMCT process. The latter species is then responsible for the observed intramolecular[74] and intermolecular HAT reactivity.[75,76] This strategy has enabled remarkable chemical transformations such as the activation of light alkanes,[75] both in batch and flow conditions.

Quite recently, however, a meticulous mechanistic analysis by Walsh and Schelter suggested the intermediacy of a chlorine radical as the key intermediate for the same transformation (Scheme 12).[77] Thus, the $CeCl_6^{2-}$ undergoes photolysis via a LMCT process triggered by UV-light irradiation to yield Cl•, which is responsible for the HAT step from **12.1** to deliver a methyl radical. Radical addition onto **12.2** produces adduct **12.4•**, which is responsible for the closure of the photocatalytic cycle. Tetraethylammonium chloride was found to increase the yield of **12.3**, however it was shown that the reaction occurred also in its absence, albeit in lower yield (43% NMR yield). As a comparison, in Zuo's original report methane (**12.1**) was converted to protected hydrazine **12.3** in 63% yield in the presence of $(Bu_4N)_2CeCl_6$ as the photocatalyst and 2,2,2-trichloroethanol as the free alcohol.

In another instance, a similar approach was adopted for the cross-dehydrogenative coupling (CDC) between alkanes and quinoxalin-2(1H)-ones or heteroarenes under air-equilibrated conditions (Scheme 13).[78] For example, when an acetonitrile solution of 1-methylquinoxalin-2(1H)-one (**13.1**) and cyclohexane (**13.2**) was irradiated with visible light (λ = 405 nm) in the presence of $CeCl_3$ as the photocatalyst, chlorine radicals were produced and the C-centered radicals obtained via HAT were trapped by **13.1** to give the expected CDC product (**13.3**, 87% yield). The authors adopted TBACl as a reservoir of chloride anions and trifluoroethanol to activate **13.1** via protonation. By replacing the alcohol with trifluoroacetic acid (TFA), also quinolines could be engaged in the desired CDC reactivity, according to a more traditional cross-dehydrogenative Minisci coupling (Scheme 13B). For example, **13.4** was alkylated in 55% yield. In both the abovementioned cases, air works as a terminal oxidant to recover the spent cerium photocatalyst and ensure the recovery of aromaticity in the products.

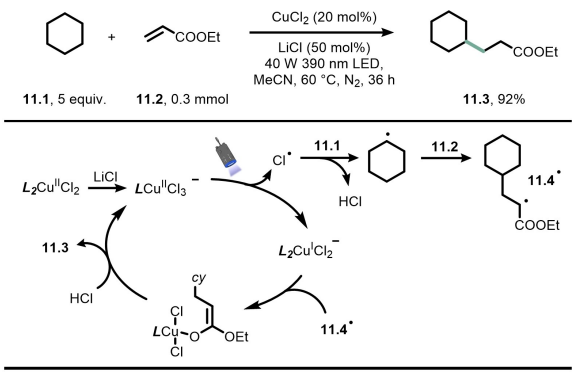

Scheme 11. Hydroalkylation of electron-poor olefins enabled by the catalytic generation of chlorine radicals via LMCT-triggered homolysis of a Cu^{II}–Cl bond.

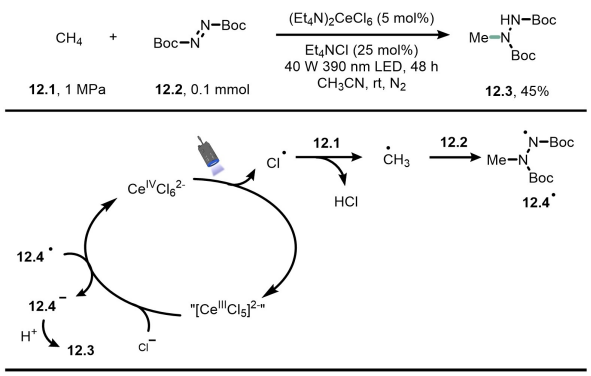

Scheme 12. Amination of light alkanes through the catalytic generation of chlorine radicals via LMCT-triggered homolysis of a Ce^{IV}–Cl bond.

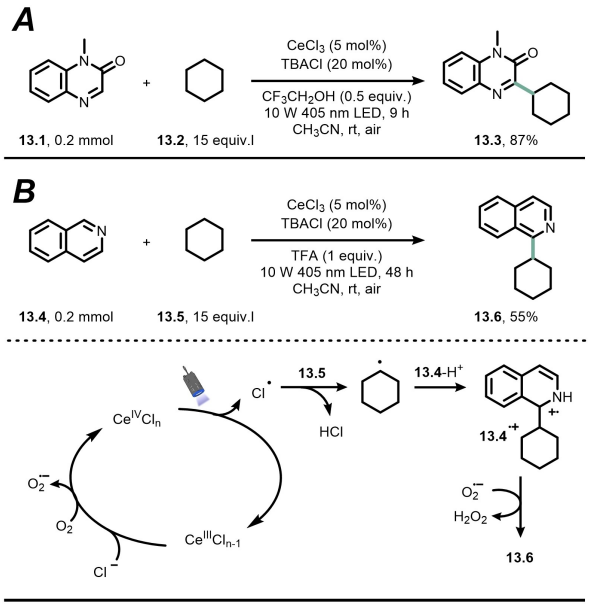

Scheme 13. Cross-dehydrogenative coupling (CDC) between alkanes and 1-methylquinoxalin-2(1H)-one (A) and isoquinoline (B) via LMCT-triggered homolysis of a Ce^{IV}–Cl bond.

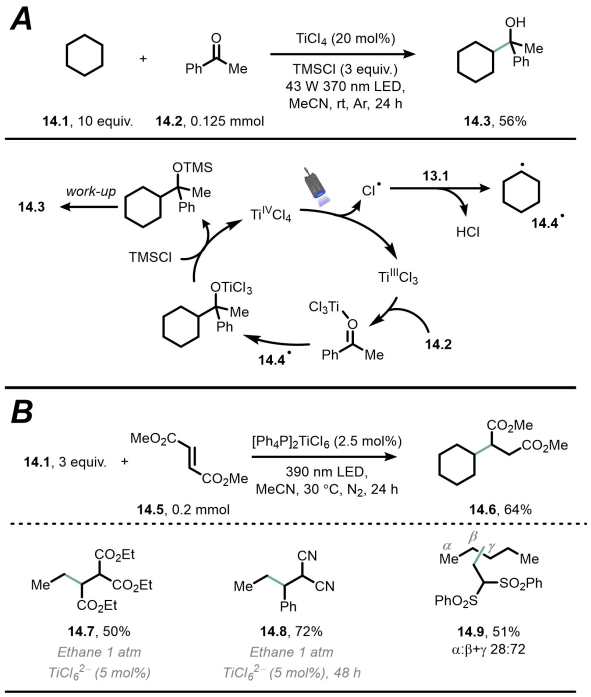

Scheme 14. A) Photoalkylation of carbonyl compounds enabled by the catalytic generation of chlorine radicals via LMCT-triggered homolysis of a Ti^{IV}–Cl bond; B) Radical hydroalkylation of olefins enabled by the catalytic generation of chlorine radicals via LMCT-triggered homolysis of a Ti^{IV}–Cl bond

2.5. Titanium

Very recently, titanium has been likewise reported to promote the generation of chlorine radicals via LMCT. In particular, Kanai and co-workers found that the irradiation ($\lambda = 370$ nm) of cheap and commercially available $TiCl_4$ in acetonitrile resulted in the formation of chlorine radicals.[79] The latter intermediates were used to cleave strong C(sp^3)–H bonds and the resulting C-centered radicals were employed for the hydroalkylation of electron-poor olefins and ketones (Scheme 14A). Thus, when an acetonitrile solution of cyclohexane (**14.1**) and acetophenone (**14.2**) is irradiated with UV light, organoradical **14.4•** is generated and readily trapped by the carbonyl compound to afford alcohol **14.3** in 56% yield after aqueous work-up. The authors found that the $TiCl_3$ species generated upon photolysis is essential to activate the carbonyl compounds towards radical addition acting as a Lewis acid. It is important to stress that the reaction required an excess of TMSCl to facilitate catalyst turnover: in its absence, the reaction did not proceed.

Walsh, Schelter and co-workers have reported a very complete study on the use of the hexachlorotitanate anion to promote the radical hydroalkylation of electron-poor olefins (Scheme 14B).[80] According to the authors, irradiation of this anion with UV light ($\lambda = 390$ nm) triggers an LMCT that results into the production of chlorine radicals and a reduced $Ti^{III}Cl_x$ species. Compared to the related $Ce^{III}Cl_x$ species (Scheme 12), $Ti^{III}Cl_x$ is much more reducing ($\Delta E_{pa} = 0.72$ V), thus enabling access to more electron-rich olefins by facilitating the reduction of the radical adduct of the Giese reaction. For example, when an acetonitrile solution of cyclohexane (**14.1**) and dimethyl fumarate (**14.2**) was irradiated with UV light in the presence of $[PPh_4]_2TiCl_6$, product **14.6** was isolated in 74% yield. Notably, the same transformation could be extended to challenging gaseous alkanes[81] such as ethane (1 atm) to obtain adduct **14.7** and **14.8** in 50% and 72% yield. The site-selectivity of the HAT step was also investigated with pentane as the substrate (see compound **14.9**) and found to be in accordance with a chlorine radical as the hydrogen abstracting species.

3. Generation of Halogen Radicals via Photoredox Catalysis

The approaches discussed in Section 1 rely on the formation of a metal halide complex and the subsequent photolysis of the M–X bond (M: metal) to generate halogen radicals for the HAT event, according to an overall inner-sphere electron transfer mechanism.[45] However, similarly to other indirect HAT methodologies (e.g. based on quinuclidines, sulfonamides, thiols etc.),[29,30] the use of an outer-sphere mechanism can be also conceived. Thus, the reductive quenching of the excited state of the photocatalyst by a halide anion leads to the formation of the targeted electrophilic halogen radicals that can be used to cleave a wide array of C(sp^3)–H bonds.

The examples reported below have been classified according to the halide being oxidized. As it can be noticed, most of them deal with the oxidation of the bromide anion, which is much more thermodynamically accessible than that of the

chloride one (see Table 1). In fact, the oxidation of Cl^- required harsher conditions and strongly oxidizing photocatalysts.

3.1. Chloride anion

Back in 2011, Fukuzumi reported the photooxygenation of C–H aliphatic bonds.[82,83] The authors found that, when an O_2-saturated solution of acetonitrile containing cyclohexane or toluene and HCl was irradiated with visible light in the presence of an acridinium photocatalyst (9-mesityl-10-methylacridinium, Acr^+–Mes), a mixture of cyclohexanol/cyclohexanone or benzaldehyde/benzoic acid was obtained. The authors proposed that chloride anion behaves as reductive quencher of the excited state of the acridinium catalyst in a single electron transfer event generating the chlorine radical. The following hydrogen abstraction leads to the formation of C-centered radicals that promptly react with oxygen to deliver the oxygenated products. Later on, Ye and co-workers exploited the same oxidative approach for the synthesis of benzocoumarins starting from 2-methyl-1,1′-biaryls compounds. In particular, the latter compounds were converted into the corresponding carboxylic acids via chlorine radical-mediated photooxygenation. Next, the carboxylic acids underwent oxidative cyclization to give coumarins.[84]

The Barriault group reported the photoredox catalytic generation of chlorine radicals for the hydroalkylation of electron-poor alkenes (Scheme 15).[85] In detail, when a benzene solution of cyclohexane (**15.1**, 3 equiv.) and dimethyl maleate (**15.2**, 0.2 mmol) was irradiated with blue light at 60 °C in the presence of an Ir-based photocatalyst having Cl^- as counterion, the hydroalkylated product **15.3** was isolated in 68% yield.

The authors noticed the formation of regioisomers in several cases, which was ascribed to the highly aggressive nature of chlorine radicals. They also found that the solvent played a key role in site-selectivity and that a coordinating solvent like pyridine allowed to achieve better selectivity towards the more thermodynamically favored positions (see also Section 5). As for the mechanism, the authors proposed that the excited state of the Ir-photocatalyst oxidizes the chloride anion to deliver the desired chlorine radical. This process is thermodynamically unfavorable ($E^{red}[Ir^{III}*/Ir^{II}] = +1.21$ V vs. SCE: $E^0[Cl^•/Cl^-] = +2.03$ V vs. SCE), which is why heating is essential for this step. Next, **15.1** is activated to afford nucleophilic alkyl radical **15.4•**, in turn trapped via radical addition onto **15.2** to give intermediate **15.5•**. The latter intermediate closes the photocatalytic cycle by re-oxidizing the photocatalyst and product **15.3** is formed upon protonation by HCl.

Later on, the same group adopted a similar Ir/Cl^- strategy to achieve the Minisci-type coupling between alcohols and ethers as radical alkylating agents.[86]

A similar methodology was independently developed by Wu and co-workers for the alkylation and allylation of C–H bonds with electron-poor alkenes in flow (Scheme 16).[87] Thus, when an acetonitrile-dichloroethane solution of cyclohexane (**16.1**, 2 equiv.) and benzalmalononitrile (**16.2**, 0.4 mmol) was irradiated under blue light in the presence of an acridinium photocatalyst and HCl as chloride source, product **16.3** was obtained in excellent yields (98%, Scheme 16A).

The methodology was efficiently applied to the alkylation of different activated and unactivated C(sp^3)–H bonds, including

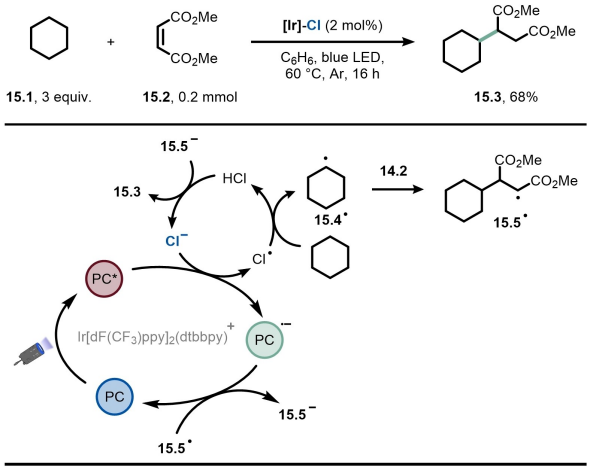

Scheme 15. Hydroalkylation of electron-poor olefins enabled by the generation of chlorine radicals via photoredox catalysis.

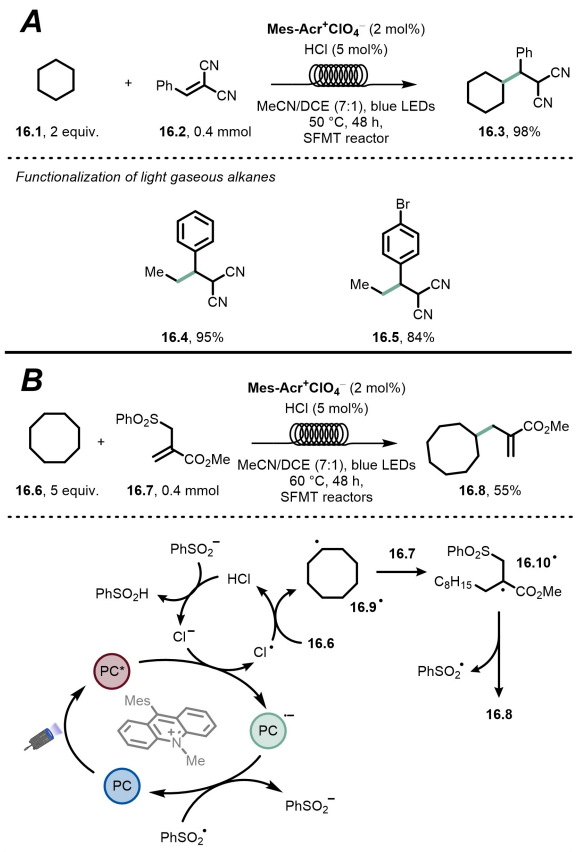

Scheme 16. A) Hydroalkylation of electron-poor olefins enabled by the generation of chlorine radicals via photoredox catalysis; B) C–H allylation via radical addition-fragmentation approach enabled by the generation of chlorine radicals via photoredox catalysis.

challenging light gaseous alkanes (see compounds **16.4** and **16.5**). The implementation of a stop-flow microtubing (SFMT) reactor was essential to prevent the HCl evaporation and effectively handle the gaseous species. Interestingly, a protocol for the allylation of C(sp^3)–H bonds using allyl phenyl sulfone as a SOMOphilic allylating agent was also reported (Scheme 16B).

Herein, the excited state of the photocatalyst is responsible for the generation of the chlorine radical via SET. Upon HAT from **16.6**, intermediate **16.9**• is generated, which is promptly intercepted by SOMOphile **16.7**. The so-formed intermediate **16.10**• undergoes fragmentation to deliver the expected allylated product (**16.8**, 55% yield) and $PhSO_2$•. The latter is entrusted for the closure of the photocatalytic cycle.

3.2. Bromide anion

In 2019, Huang and coworkers reported that the presence of LiBr could speed up the photoredox Minisci-type alkylation of quinoline derivatives using ethers as coupling partners (Scheme 17A).[88] Thus, when a wet chlorobenzene solution containing tetrahydrofuran (**17.1**, 4 equiv.), 4-methylquinoline (**17.2**, 0.2 mmol), LiBr and triflic acid as additives was irradiated with blue light in presence of an iridium photocatalyst, product **17.3** was isolated in 90% yield. Interestingly, HBr could be used both as bromide source and proton source without compromising the reactivity (79% yield).

The authors proposed that Br•, generated upon reductive quenching of the excited state of the iridium photocatalyst by the bromide anion, performs HAT on tetrahydrofuran. The so-formed radical **17.4**• is readily intercepted by protonated **17.2** to deliver intermediate **17.6**• via the intermediacy of **17.5**•+. A Spin-Center Shift (SCS) and subsequent ring opening of the ether affords benzyl radical **17.7**•, which is entrusted for the closure of the photocatalytic cycle.

Later on, the same group adopted a similar system for the bromine-mediated alkylation of quinolines and quinazolinones using different hydrogen donors such as aldehydes[89,90] and ester acetates (Scheme 17B).[91] Very recently, the group has developed a decarbonylative strategy to accomplish the hydroalkylation of acrylamides with aldehydes.[92]

Quite recently, Murakami and co-workers developed a cross-dehydrogenative coupling between benzylic and aldehydic C–H bonds (Scheme 18).[93] Thus, when an ethyl acetate

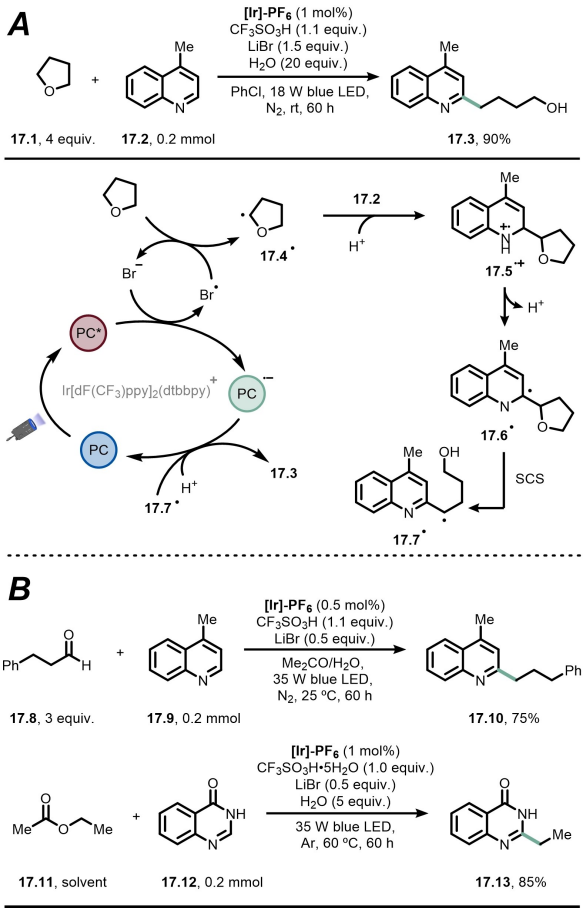

Scheme 17. A) Minisci-type coupling of N-heteroarenes with ethers enabled by the generation of bromine radicals via photoredox catalysis; B) Minisci-type coupling of N-heteroarenes with aldehydes and ester acetates enabled by the generation of bromine radicals via photoredox catalysis. SCS: Spin-Center Shift.

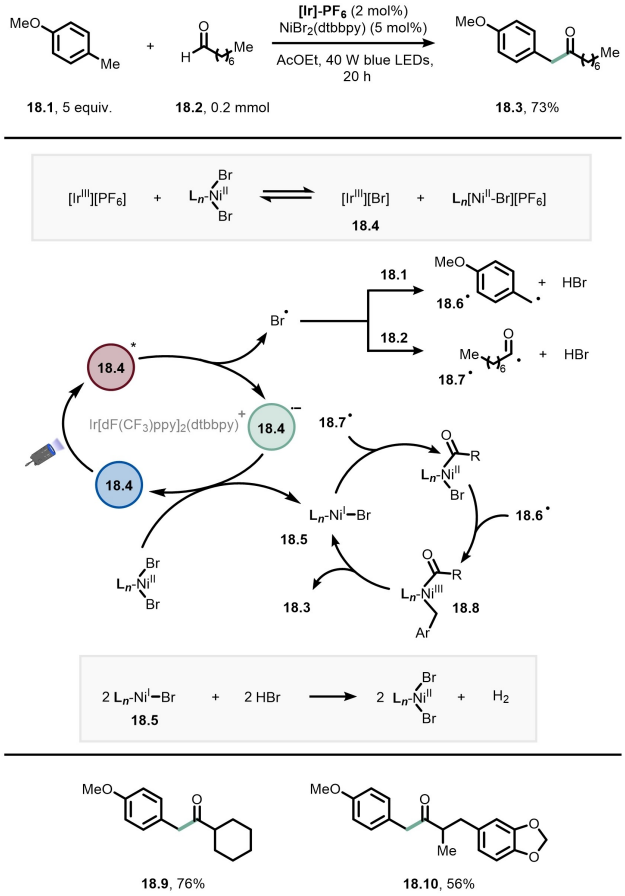

Scheme 18. Photoinduced cross-dehydrogenative coupling between aldehydes and alkyl arenes enabled by the generation of bromine radicals via photoredox catalysis.

solution of 4-methoxytoluene (**18.1**, 5 equiv.) and octanal (**18.2**, 0.2 mmol) was irradiated with a blue LED in the presence of an Ir-based photocatalyst and $NiBr_2$(dtbbpy), the corresponding ketone **18.3** was obtained in 73% yield. As for the mechanism, an initial anion exchange between the iridium photocatalyst and the nickel co-catalyst occurs to yield **18.4**. The reductive quenching of the excited state of the latter generates the bromine radical. At this stage, another nickel complex accepts an electron from the spent photocatalyst, delivering Ni^{I} complex **18.5**. Meanwhile, the bromine radical performs hydrogen abstraction from both **18.1** and **18.2** to afford the benzyl radical **18.6•** and the acyl radical **18.7•**, respectively. These fleeting intermediates are intercepted by **18.5** to give Ni^{III} complex **18.8**. Eventually, reductive elimination yields the cross-coupled product **18.3** and complex **18.5**. Hydrogen evolution via the reaction between **18.5** and HBr restores the nickel catalyst. If on one side the cross-coupling did not work with electron-poor alkyl arenes, on the other side α-branched aldehydes gave the corresponding products in good results despite the more marked steric hindrance (see compounds **18.9–18.10**). A similar approach was also used for the dehydrogenative homocoupling of benzylic C–H bonds.[94]

The same group reported also two dehydrogenative strategies based on the generation of bromine radicals for the synthesis of esters by coupling primary alcohols or aldehydes with phenols.[95,96]

Recently, a similar approach for the dehydrogenative coupling of aldehydes and alkyl arenes in flow was reported.[97] The use of a photo-flow reactor enabled the authors to shorten the reaction times (from 20 h to 120 min) and increase the productivity up to 10.5 $g \cdot day^{-1}$. Furthermore, the method is efficient for the late-stage functionalization of interesting API like celecoxib and metaxalone.

The Huo group gave an important contribution to the field of photoredox-generated halogen radicals for HAT by reporting several enantioselective transformations based on bromine radicals.[98–101] In one of these examples, the enantioselective acylation of α-to-N $C(sp^3)$–H bonds using ubiquitous carboxylic acids as acylating partner to produce α-amino ketones was reported (Scheme 19).[98] In detail, when an isopropyl acetate solution of acetic acid (**19.1**, 0.1 mmol) and *N*-pentyl benzamide (**19.2**, 3.0 equiv.) was irradiated with a blue LED in the presence of an Ir-based photocatalyst, $NiBr_2 \cdot$glyme, a chiral ligand **19.4**, dimethyl dicarbonate (DMDC) and a base, the corresponding α-amino ketone **19.3** was obtained in 88% yield and 90% *ee*. The method tolerated a variety of functional groups and could be used for the late-stage functionalization of natural products (**19.9–19.11**). As for the mechanism, Ni^0 undergoes oxidative addition onto the in situ-formed acyl electrophile **19.5** to give the acyl-Ni^{II} species **19.7**. In the meantime, the bromide acts as quencher of the excited state of the photocatalyst to give the bromine radical, which abstracts a hydrogen atom from **19.2** to deliver the α-amino radical **19.6•**. The last is captured from **19.7** to deliver the Ni^{III} species **19.8**, which undergoes reductive elimination to afford the product **19.3** and Ni^{I} complex. Finally, the photocatalytic cycle is closed by the single electron reduction of Ni^{I} by the exhausted photocatalyst.

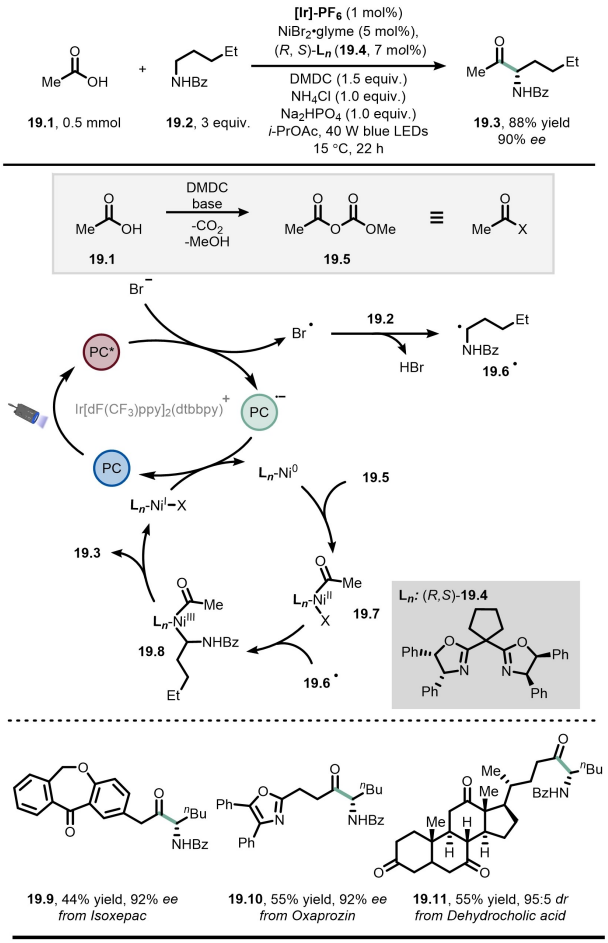

Scheme 19. Enantioselective acylation of N-alkyl benzamides for the synthesis of α-amino ketones enabled by the generation of bromine radicals via photoredox catalysis. DMDC: dimethyl dicarbonate.

In another very recent instance, Deng and co-workers have reported a photoinduced, bromine radical-based monofluoroalkenylation of $C(sp^3)$–H bonds in batch and flow (Scheme 20).[102] In detail, when a tetrahydrofuran solution of 2-(2,2-difluorovinyl)naphthalene (**20.1**, 0.2 mmol) was irradiated with a blue LED in the presence of an Ir-based photocatalyst, tetrabutylammonium bromide (TBABr) as bromine source and $NaHCO_3$ as the base, product **20.2** was isolated in 79% yield (*E:Z* 1:1) after 24 h. The reaction was efficiently translated in flow and scaled up to 1.05 g over an operation time of 15 h. As discussed above, the reductive quenching of the excited state of the Ir photocatalyst by the bromide anion generates the bromine radical that performs HAT from tetrahydrofuran to give the radical **20.3•**. The single electron reduction of **20.1** by the reduced form of Ir-photocatalyst closes the photocatalytic cycle and affords the fluoroalkenyl radical **20.4•** via the defluorination of the radical anion intermediate **20.1•⁻**. Eventually, the radical-radical coupling between **20.3•** and **20.4•** delivers the final product **20.2**.

In another case, the Doyle group described an Ir/Ni dual catalytic protocol to reach the methylation and alkylation of

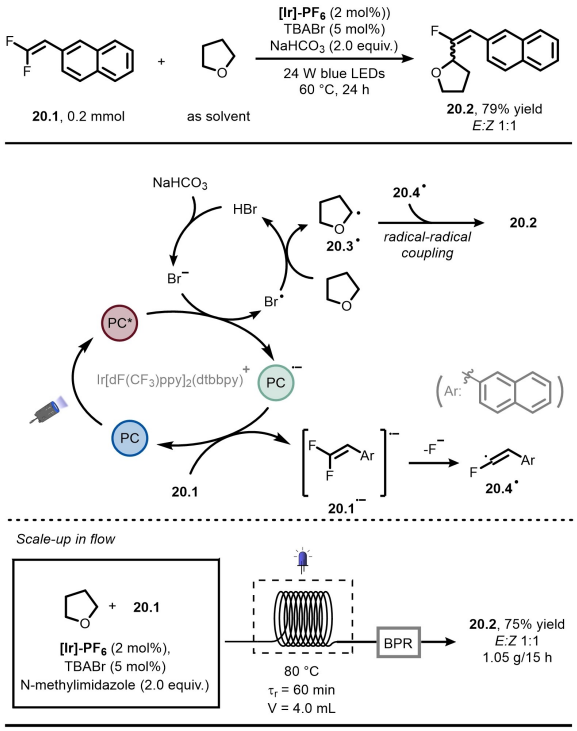

Scheme 20. Photoinduced monofluoroalkenylation of C(sp^3)–H bonds enabled by the generation of bromine radicals via photoredox catalysis.

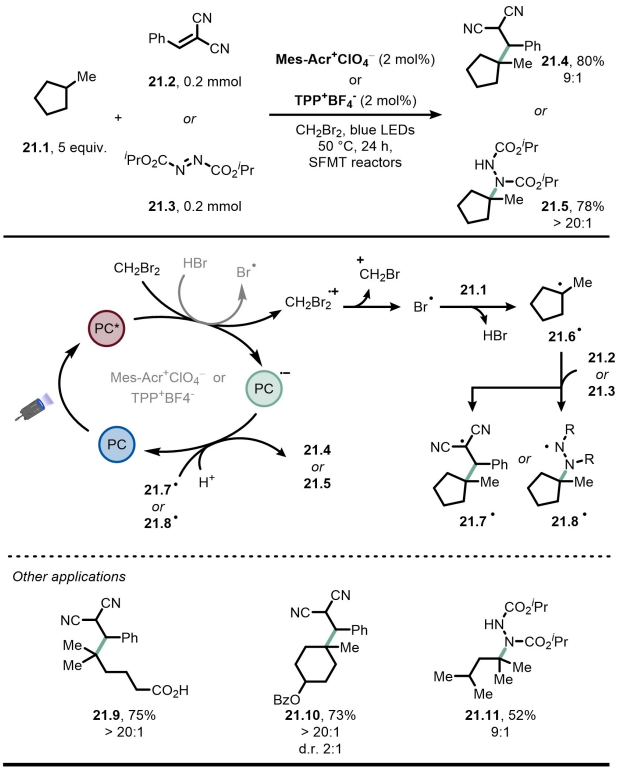

Scheme 21. Hydroalkylation of electron-poor olefins enabled by the generation of bromine radicals from dibromomethane via photoredox catalysis.

aryl halides using benzaldehyde di-alkyl acetals as carbon-centered radical sources.[103] The generation of a bromine radical is proposed to mediate the HAT with the benzaldehyde di-alkyl acetates. Interestingly the authors employ data science tools to explore the chemical space of commercially available aryl bromides and possibly predict unreactive patterns in the methodology.

Recently, the Wu group disclosed CH_2Br_2 as bromine radical source (Scheme 21) for the selective functionalization of unactivated tertiary C(sp^3)–H bonds.[104] Thus, a dibromomethane solution of methylcyclopentane (**21.1**, 5 equiv.) and benzalmalononitrile (**21.2**, 0.2 mmol) or diisopropyl azodicarboxylate (**21.3**, 0.2 mmol) was irradiated with a 18 W blue LED strip at 50 °C in a stop-flow microtubing reactor (SMFT). Thanks to the presence of mesityl acridinium (Mes-Acr^+) or 2,4,6-triphenylpyrylium (TPP^+) photocatalysts, products **21.4** and **21.5** were obtained in 80% and 78% yield, respectively, with high preference for the tertiary C–H bonds. The authors ascribe the selectivity to the low BDE value of H–Br (87 kcal/mol, see Table 1). As for the mechanism, the authors reported that the employment of strongly oxidative photocatalysts is required to promote the single electron oxidation of CH_2Br_2 ($E_{1/2}^{ox} = +1.62$ V versus SCE) to the corresponding radical cation. DFT calculation demonstrated that CH_2Br_2 radical cation preferentially decomposes generating bromomethyl cation and bromine radical. The latter performs hydrogen abstraction from **21.1** to generate **21.6•**, which is readily intercepted by **21.2** or **21.3** to give the electrophilic radical **21.7•** or **21.8•**, respectively. Finally, the latter intermediates are entrusted for the closure of the photocatalytic cycle. The authors observed that HBr is produced over the course of the reaction, which might compete with CH_2Br_2 as a more efficient bromine radical source.

4. Generation of Halogen Radicals via Energy Transfer

Another mechanism that can be exploited to photocatalytically generate halogen atoms for indirect HAT is based on energy transfer (EnT).[105] In this manifold, the photocatalyst is typically an iridium photocatalyst and is in charge of absorbing light and transferring energy to a Ar–Ni^{II}–X species generated upon oxidative addition onto aryl halides. It is important to remark that a Ni^{III} species is not involved here. The examples in this section have been gathered according to the transformation performed.

In 2016, Molander and co-workers reported the first C–H arylation protocol based on this concept.[106] Thus, when a tetrahydrofuran solution of aryl bromide **22.1** (0.35 mmol) was irradiated with a Compact Fluorescent Lamp in the presence of 4,4′-dimethoxybenzophenone, an Ir-based photocatalyst, Ni-$(NO_3)_2$ hexahydrate and 4,4′-di-tert-butyl-2,2′-bipyridine (**22.3**), product **22.2** was obtained in 75% yield after 2 days (Scheme 22A). The presence of the diaryl ketone was found to accelerate the reaction, however it was not essential. As for the mechanism, the in situ-generated Ni^0 species undergoes oxida-

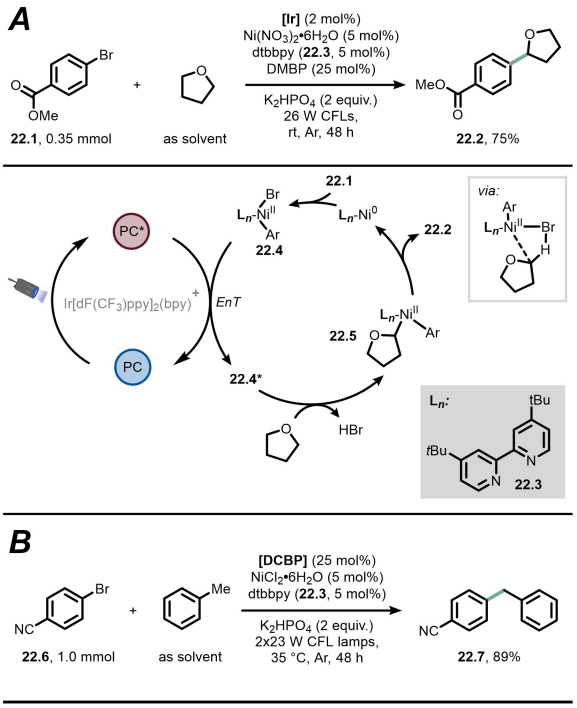

Scheme 22. A) Arylation of C–H bonds via the catalytic generation of bromine radicals via energy transfer to a nickel complex. B) Bromine-radical-mediated arylation of benzylic C(sp^3)–H bonds via the catalytic generation of bromine radicals via energy transfer to a nickel complex. DCBP: 4,4′-dichlorobenzophenone.

tive addition onto **22.1** to produce an Ar–Ni^{II}–Br species (**22.4**) that is photosensitized by the iridium photocatalyst. **22.4*** interacts with tetrahydrofuran in a concerted, four-centered transition structure to deliver intermediate **22.5** via σ-bond metathesis. Finally, reductive elimination affords the expected product **22.2** and recovers the Ni^0 species, prone to start a new cycle. To actually prove that an EnT was occurring, the authors showed that the same reaction could be performed by directly irradiating the nickel complex in the UV region in the absence of the photosensitizer.

In another instance, the Rueping group reported the arylation of benzylic C(sp^3)–H bonds.[107] Thus, the irradiation of a toluene solution of aryl bromide **22.6** with CFLs in the presence of 4,4′-dichlorobenzophenone (DCBP), $NiCl_2 \cdot 6H_2O$ (and dtbbpy as the ligand) and K_2HPO_4 delivered the arylated product **22.7** in 89% yield on 1 mmol scale (Scheme 22B). As for the mechanism, the authors predicted that the benzophenone would act as a hydrogen atom transfer photocatalyst to activate the alkyl aromatic compound. The resulting compound would be captured by the nickel catalytic cycle to deliver product **22.7**. However, when testing aryl iodides, which should be more prone to oxidative addition by nickel, the yields dropped. Intriguingly, reactivity was restored by adding one extra equivalent of TBABr. This led the authors to propose a parallel mechanistic picture, where the diaryl ketone works as a photosensitizer for the Ar–Ni^{II}–Br complex, which then liberates a bromine radical that is in turn responsible for the HAT step. Interestingly, the same methodology was extended to a limited set of aryl chlorides.

A similar strategy was adopted by König and colleagues for the arylation of the α-to-N position of tertiary amides as well as ureas by using mesoporous graphitic carbon nitride (mpg-CN) as the photosensitizer (Scheme 23).[108] Notably, this is the first report of the use of this organic semiconductor in this role. Thus, mpg-CN absorbs visible light (450 nm) and sensitizes the Ar–Ni^{II}–X species (X: halide) generated upon oxidative addition onto aryl halide **23.1 a** or **23.1 b**. The abovementioned halogen atom photoelimination-HAT-radical rebound-reductive elimination sequence afforded the expected benzyl amide **23.2** in excellent yields (89% when X = Cl, 85% when X = Br). It is interesting to note that when *N*,*N*′-dimethylpropylene urea (**23.3**, DMPU) was used as the substrate, the CH_3 group was primarily functionalized when 4-chloroacetophenone was used as the coupling partner. Conversely, when 4-bromoacetophenone was used, the methylene group was preferentially arylated. A competitive LMCT-based mechanism (see Section 1.1) was ruled out based on a stoichiometric experiment where an Ar–Ni^{II}–X was irradiated (450 nm) in the presence of *N*,*N*-dimethylacetamide in the absence of mpg-CN. Even though in lower yield, the expected product could be detected, thus demonstrating the involvement of an excited Ni^{II} species. This approach was also suitable for the manipulation of bioactive molecules such as cholesterol and D-Glucose diacetonide (compounds **23.4** and **23.5**).

Rueping and co-workers reported the cross-coupling of allylic C(sp^3)–H bonds with aryl and vinyl bromides (Scheme 24), where β-bromostyrene **24.1** (0.2 mmol) was reacted with tetramethylethylene (**24.2**, 10 equiv.) in the presence of [Acr-Mes]ClO_4 and $NiCl_2$·glyme (and **24.4** as the ligand) under blue light irradiation to obtain product **24.3** in 53% yield with

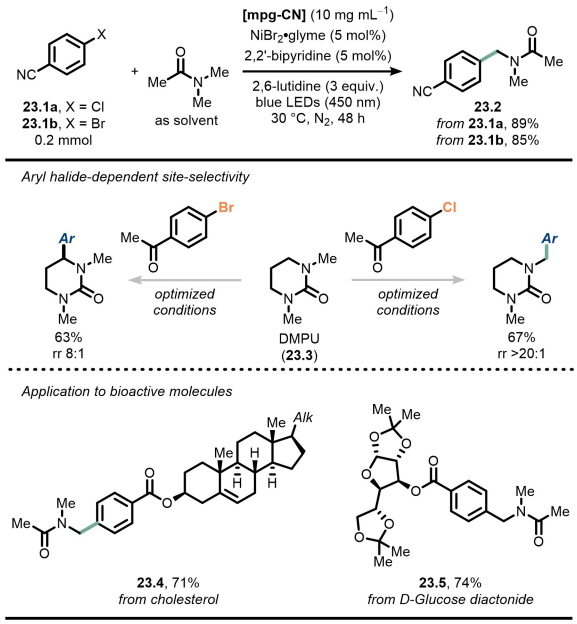

Scheme 23. Arylation of α-to-N C–H bonds of tertiary amides and ureas via the generation of bromine radicals via energy transfer to a nickel complex.

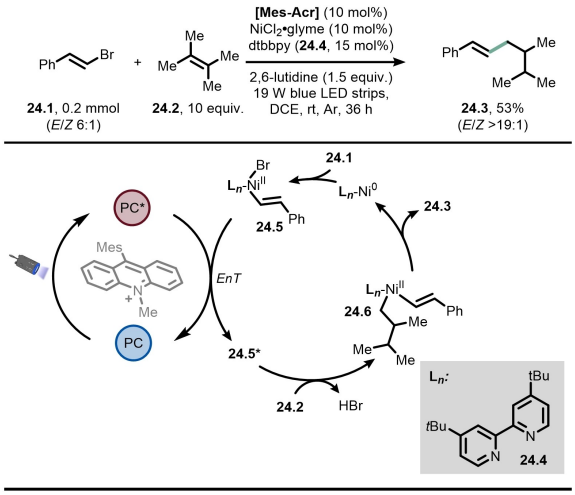

Scheme 24. Cross-coupling of allylic C(sp^3)–H bonds with vinyl bromides via the catalytic generation of bromine radicals via energy transfer to a nickel complex. Mes: mesityl.

exquisite *E* diasteroselectivity.[109] According to the authors, the excited state of the acridinium catalyst can sensitize a vinyl–Ni^{II}–Br (**24.5**) moiety generated upon oxidative addition of a Ni^0 species onto **24.1**. At this stage, a bromine radical is produced and is responsible for HAT from **24.2** and the resulting radical intermediate is rapidly captured by the nickel center to afford **24.6**. Finally, reductive elimination from the latter complex affords the hoped-for product together with the Ni^0 species. The very same conditions could be extended to aryl bromides and aryl iodides, the latter requiring LiBr as an additive to provide the required bromide ion.

Later on, Shibasaki and colleagues reported the α-acylation of ethers (Scheme 25).[110] In detail, when a tetrahydrofuran solution of acyl chlorides **25.1** was irradiated in the presence of an Ir-based photosensitizer, $NiCl_2$ and 4,4′-di-tert-butyl-2,2′-bipyridine, the corresponding acylated product **25.2** was obtained in 85% (dr 1:1). The proposed mechanism is similar to that proposed by Molander (reported in Scheme 22A) and starts with oxidative addition of an in situ-generated Ni^0 species onto **25.1**. The so-formed Ni^{II} species is sensitized by the Ir-photocatalyst and chlorine radical photoelimination occurs. After HAT

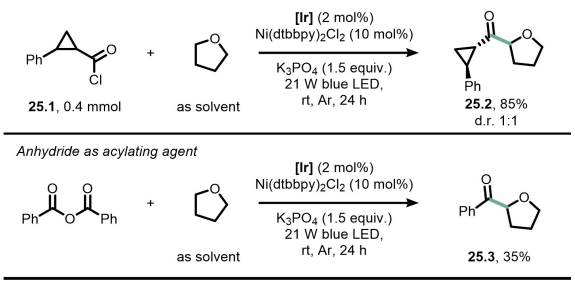

Scheme 25. α-Acylation of ethers via the catalytic generation of chlorine radicals via energy transfer to a nickel complex.

from the ether (used as the solvent), radical rebound and reductive elimination, the catalytic cycle of nickel is closed. Also anhydrides were suitable partners under these conditions (compound **25.3**, 35%), however the product was obtained in modest yields.

5. Miscellaneous

This section gathers a limited set of examples that rely on indirect HAT by a halogen atom but do not fit any of the abovementioned categories (Sections 1–3).

In one instance, Lu and co-workers reported the enantioselective arylation of benzylic C(sp^3)–H bonds by adopting an Ir/Ni dual catalytic strategy (Scheme 26).[111] Although in the majority of cases shown above, a LMCT in a fleeting Ni^{III}–Cl species is proposed, in this case the authors proposed a different scenario. Thus, when a solution of aryl bromide **26.1** in dioxane/ethyl benzene 3:1 was irradiated with blue light in the presence of an Ir-photocatalyst, $NiCl_2 \cdot DME$, bisimidazoline **26.3** as the chiral ligand and 4,4′-dimethoxybenzophenone (DMBP), product **26.2** was obtained in 84% (91% *ee*) after isolation. The authors proposed that Ni^0 undergoes oxidative addition onto the aryl bromide. The so-formed Ar–Ni^{II}–Br species is oxidized by the excited state of the photocatalyst to directly provide the bromine atom for HAT from ethyl benzene. Radical capture of the C-centered radical, reductive elimination to give **26.2** and reduction by the spent photocatalyst are needed to close the catalytic cycle of the nickel. It is important to stress, however, that despite the authors did not consider the LMCT-triggered photolysis of an in situ-generated Ni^{III}–Br species, they did not rule out the possibility of an energy transfer (see Section 3).

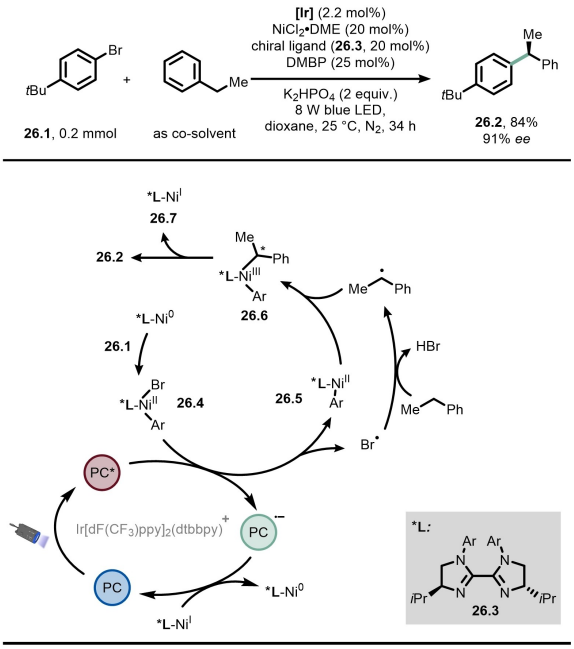

Scheme 26. Bromine-radical-mediated enantioselective arylation of benzylic C–H bonds.

By adopting a similar strategy, the same group reported the stereo and enantioselective alkenylation of benzylic C–H bonds.[112] As above, the authors proposed that the oxidation of the alkenyl-Ni^{II}-Br by the excited state of the Ir-photocatalyst affords the free bromine radical for hydrogen abstraction from a benzylic C–H bond.

Murakami and co-workers reported the benzylic C–H arylation of alkyl aromatics.[113] Overall, compared to other reports mentioned above, this approach did not require a dual catalytic system. The authors proposed that a Ni^{I} species is generated in situ from the bench-stable Ni^{II} catalyst via a photoinduced electron transfer from the alkyl aromatic to the metal complex. Next, oxidative addition onto the aryl bromide affords an Ar–Ni^{III}–Br species, which undergoes photolysis under UV light to deliver a bromine radical. Indirect HAT, radical capture and reductive elimination affords the product together with a Ni^{I} species, ready to start a new catalytic cycle.

6. Steering site-selectivity of halogen radical-mediated Hydrogen Atom Transfer

As mentioned in the introduction, halogen radical-mediated HAT has been traditionally tagged in synthetic endeavors as an unselective process, at least as far as $Cl^{\bullet}$ is concerned. As a matter of fact, while bromine atoms somehow allow for discrete levels of site-selectivity due to the lower BDE of the H–Br bond (see Table 1), a H–Cl bond is much stronger, providing a considerably higher thermodynamic force for hydrogen abstraction.[114] Furthermore, the greater selectivity of bromine-mediated HAT can be explained based on the fact that this is an endergonic process. Thus, according to the Hammond postulate, the reaction features a "late" transition state with a marked radical character on the carbon atom. The more stabilized the nascent alkyl radical, the higher the selectivity. On the contrary, chlorine-mediated HAT is an exergonic process with an "early" transition state where the carbon atom has a smaller radical character. Hence, even though the stability of the nascent alkyl radical is still important to justify the final outcome, it plays a less decisive role, thus causing a decreased selectivity.

This results into the nearly indiscriminate activation of different C–H bonds within a molecule (Scheme 27A). However, there is a significant body of literature illustrating the possibility to tune the site-selectivity of Cl-mediated HAT event via the judicious choice of additives and solvents.[115–119]

In one instance, Barriault and co-workers performed the hydroalkylation of electrophilic olefins by using a photoredox approach, as already shown in Scheme 15.[85] Despite the generality of such approach, the authors consistently obtained mixtures of products deriving from the functionalization of different positions (primary, secondary or tertiary C–H bonds) within the substrates. Accordingly, they became interested in channeling the reactivity of $Cl^{\bullet}$ towards the more thermodynamically favored tertiary position. As it is known that the use of solvents can attenuate the high reactivity of chlorine atoms for hydrogen abstraction,[115–119] they investigated the effect of several solvents on the reaction outcome and found that pyridine could increase the selectivity towards the tertiary position. Thus, when substrate **27.1** was subjected to optimized conditions described above, the ratio of tertiary:primary activation was found to be 3:1 (59% yield overall). However, when pyridine was adopted as the solvent, the ratio increased to 9:1 and even further (10:1) when the concentration was lowered. These results confirm a heavy dependency of the site-selectivity of chlorine-mediated hydrogen abstraction on the solvent (see Scheme 27B).

Another interesting case was offered by Walsh and Schelter in their study on $CeCl_6^{2-}$ as a source of $Cl^{\bullet}$ via LMCT (Scheme 27C).[77] The authors addressed the selectivity issue by adopting 2,3-dimethylbutane (**27.2**) as a substrate for the reaction of interest and set out to compare the tertiary vs primary functionalization. They found that the tertiary:primary activation ratio could be significantly modified by adding a suitable co-solvent. Thus, when the reaction was performed under optimized conditions in neat acetonitrile, the ratio was found to be 51:49; however, by adding *t*BuOH (4 M), the ratio increased to 69:31, and when the same concentration of benzene was added, the ratio increased even further to 81:19. The authors also proved that, upon increasing the concentration of the additive, they could force the complexation of the photogenerated chlorine radical and achieve higher levels of selectivity.

More recently, Nocera and colleagues managed to go towards the opposite direction and shift the selectivity away from more thermodynamically accessible tertiary positions by capitalizing on steric hindrance (Scheme 27D).[114] In detail, they demonstrated that $Cl^{\bullet}$, photoeliminated from an Fe^{III} chloride pyridinediimine (PDI) complex via LMCT, can be confined by the secondary coordination sphere of the metal complex itself. This interaction creates a bulky $Cl^{\bullet}|$arene complex that possesses a considerable steric hindrance compared to the free chlorine atom. This enabled the photochemical C(sp^3)–H chlorination and bromination that were more selective for sterically accessible primary and secondary C–H bonds, overriding thermodynamic preference for weaker tertiary C–H bonds. Interestingly, the authors found that the addition of benzene to the reaction mixture led to a loosening of the $Cl^{\bullet}|$arene complex, which resulted in a restoration of functionalization on the tertiary position.

7. Conclusions

In conclusion, in this minireview, we have presented recent examples of synthetic applications of photocatalyzed halogen radical-mediated HAT. Three main mechanisms have been proposed in the literature: light-triggered inner-sphere single-electron transfer (*also known as* LMCT, Section 1), photoredox catalyzed outer-sphere single-electron transfer (Section 2) and energy transfer (Section 3).

The first mechanism relies on a first complexation step between the halide anion and a metal center, followed by the

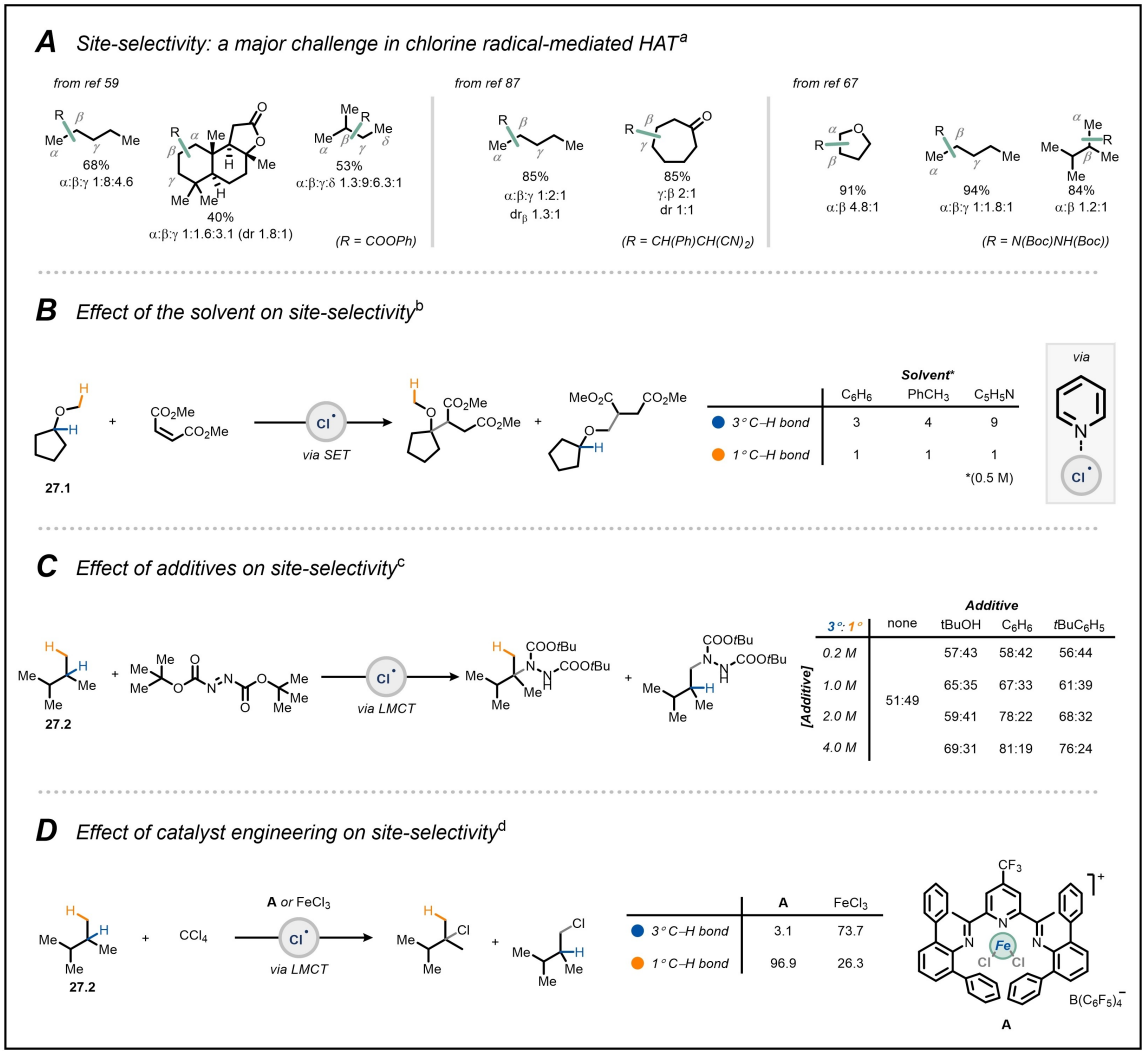

Scheme 27. A) Examples of regioselectivity issues caused by the highly aggressive chlorine radical, a mighty yet unselective hydrogen atom abstractor; B) Barriault's hydroalkylation of electron-poor olefins enabled by the generation of chlorine radicals via photoredox catalysis: the role of solvent on regioselectivity; C) Walsh's and Schelter's amination of light alkanes based on the catalytic generation of chlorine radicals via LMCT-triggered homolysis of a Ce^{IV}–Cl bond: the role of additives on regioselectivity; D) Nocera's seminal report showing how catalyst engineering can enforce steric control over chlorine-radical-mediated C–H activation. [a] data taken from refs. [59,67,87] [b] from ref. [85] [c] from ref. [77] [d] from ref. [114]

electron transfer step. This approach has been used with several metals such as Ni, Cu, Fe, Ce, Ti and the details of the mechanism can vary based on the metal center (see above). On the one hand, Ni stands out because of its unique mode of action (oxidative addition, reductive elimination), allowing to forge a wide array of C(sp^3)–C(sp^2) bonds. On the other hand, it often requires the H-donor to be used as the (co)solvent. Conversely, C(sp^3)–C(sp^3) bond formation can be conveniently achieved via radical hydroalkylation mediated by Fe, Ce, Cu or Ti.

As for the second mechanism, strongly oxidizing photocatalysts are required for the oxidation of chloride, while bromide is much more thermodynamically accessible (Table 1). However, this has a trade-off: bromine radical is not suitable for the activation of strong C–H bonds (>90 kcal mol^{-1}), while chlorine radical behaves as a mighty (yet unselective) hydrogen abstractor.

Finally, energy transfer holds great potential for the synthesis of C(sp^3)–C(sp^2) bonds and mainly relies on dual catalytic strategies based on Ni.

Despite the fact that free halogen atom-mediated HAT is often regarded as an uncontrollable process with little synthetic value, it has been shown herein that the photocatalytic generation of these highly aggressive fleeting intermediates can be considered a game-changer. Moreover, Scheme 27 exemplifies how selectivity can be tuned, at least to some extent, by carefully adjusting reaction conditions: coordinating solvents, reaction additives and catalyst engineering proved to be valuable strategies in this regard. More efforts are expected in this direction in the next future.

Finally, it can be interesting to compare halogen radicals with their S-, N- and O-based congeners, at least from a qualitative point of view. In the first instance, these are all electrophilic hydrogen abstractors, which makes them selective for the abstraction of hydridic C–H bonds to yield nucleophilic alkyl radicals. Conversely, (ligated) B-centered radicals[33] are nucleophilic in nature and can be used for the generation of electrophilic alkyl radicals.[32] RS$^{\bullet}$ and Br$^{\bullet}$ are weak abstractors and the site-selectivity observed in these cases is also influenced by Bond Dissociation Energies: the S–H (e.g., for thioglycolate)[120] and Br–H bonds are relatively weak (~ 88 kcal mol^{-1}), offering an insufficient driving force for the activation of strong aliphatic C(sp^3)–H bonds. This issue can be, at least in principle, addressed with O-, N- centered radicals and Cl$^{\bullet}$, known to be much stronger abstractors. It is extremely important to stress, however, that predicting site-selectivity in HAT is a challenging task as many factors must be taken into account.

We hope this review may bolster renewed interest from the synthetic community in the described manifold as well as stimulate mechanistic studies to better understand and finally tame these reactive intermediates.[121]

Acknowledgements

We are grateful to have received generous funding from the European Union H2020 research and innovation program under the Marie S. Curie Grant Agreement (HAT-TRICK, No 101023615, L.C.; PhotoReAct, No 956324, S.B. & T.N.).

Conflict of Interest

The authors declare no conflict of interest.

Keywords: Energy transfer · Hydrogen atom transfer · Halogens · LMCT · Photoredox catalysis

[1] J. M. Mayer, *Acc. Chem. Res.* **2011**, *44*, 36–46.
[2] W. Lai, C. Li, H. Chen, S. Shaik, *Angew. Chem. Int. Ed.* **2012**, *51*, 5556–5578; *Angew. Chem.* **2012**, *124*, 5652–5676.
[3] P. R. D. Murray, J. H. Cox, N. D. Chiappini, C. B. Roos, E. A. McLoughlin, B. G. Hejna, S. T. Nguyen, H. H. Ripberger, J. M. Ganley, E. Tsui, N. Y. Shin, B. Koronkiewicz, G. Qiu, R. R. Knowles, *Chem. Rev.* **2022**, *122*, 2017–2291.
[4] R. G. Agarwal, S. C. Coste, B. D. Groff, A. M. Heuer, H. Noh, G. A. Parada, C. F. Wise, E. M. Nichols, J. J. Warren, J. M. Mayer, *Chem. Rev.* **2022**, *122*, 1–49.
[5] S. Hammes-Schiffer, A. A. Stuchebrukhov, *Chem. Rev.* **2010**, *110*, 6939–6960.
[6] C. Chatgilialoglu, A. Studer, Eds., *Encyclopedia of Radicals in Chemistry, Biology and Materials*, John Wiley & Sons, Ltd, Chichester, UK, **2012**.
[7] L. Capaldo, L. L. Quadri, D. Ravelli, *Green Chem.* **2020**, *22*, 3376–3396.
[8] L. Capaldo, D. Ravelli, M. Fagnoni, *Chem. Rev.* **2022**, *122*, 1875–1924.
[9] M. Salamone, M. Bietti, *Acc. Chem. Res.* **2015**, *48*, 2895–2903.
[10] M. Milan, M. Salamone, M. Costas, M. Bietti, *Acc. Chem. Res.* **2018**, *51*, 1984–1995.
[11] M. Galeotti, M. Salamone, M. Bietti, *Chem. Soc. Rev.* **2022**, *51*, 2171–2223.
[12] M. A. Theodoropoulou, N. F. Nikitas, C. G. Kokotos, *Beilstein J. Org. Chem.* **2020**, *16*, 833–857.
[13] Y. R. Luo, *Comprehensive Handbook of Chemical Bond Energies*, CRC Press, **2007**.
[14] M. Finn, R. Friedline, N. K. Suleman, C. J. Wohl, J. M. Tanko, *J. Am. Chem. Soc.* **2004**, *126*, 7578–7584.
[15] M. Salamone, M. Galeotti, E. Romero-Montalvo, J. A. Van Santen, B. D. Groff, J. M. Mayer, G. A. Dilabio, M. Bietti, *J. Am. Chem. Soc.* **2021**, *143*, 11759–11776.
[16] M. Bietti, G. A. Dilabio, O. Lanzalunga, M. Salamone, *J. Org. Chem.* **2010**, *75*, 5875–5881.
[17] M. Salamone, M. Bietti, *Synlett* **2014**, *25*, 1803–1816.
[18] H. Yi, G. Zhang, H. Wang, Z. Huang, J. Wang, A. K. Singh, A. Lei, *Chem. Rev.* **2017**, *117*, 9016–9085.
[19] C. R. J. Stephenson, T. P. Yoon, D. W. C. MacMillan, *Visible Light Photocatalysis in Organic Chemistry*, Wiley-VCH Verlag GmbH & Co. KGaA, Weinheim, Germany, **2017**.
[20] I. K. Sideri, E. Voutyritsa, C. G. Kokotos, *Org. Biomol. Chem.* **2018**, *16*, 4596–4614.
[21] F. Juliá, T. Constantin, D. Leonori, *Chem. Rev.* **2022**, *122*, 2292–2352.
[22] N. Holmberg-Douglas, D. A. Nicewicz, *Chem. Rev.* **2022**, *122*, 1925–2016.
[23] S. P. Pitre, L. E. Overman, *Chem. Rev.* **2022**, *122*, 1717–1751.
[24] M. J. Genzink, J. B. Kidd, W. B. Swords, T. P. Yoon, *Chem. Rev.* **2022**, *122*, 1654–1716.
[25] J. Großkopf, T. Kratz, T. Rigotti, T. Bach, *Chem. Rev.* **2022**, *122*, 1626–1653.
[26] K. P. S. Cheung, S. Sarkar, V. Gevorgyan, *Chem. Rev.* **2022**, *122*, 1543–1625.
[27] A. Y. Chan, I. B. Perry, N. B. Bissonnette, B. F. Buksh, G. A. Edwards, L. I. Frye, O. L. Garry, M. N. Lavagnino, B. X. Li, Y. Liang, E. Mao, A. Millet, J. V. Oakley, N. L. Reed, H. A. Sakai, C. P. Seath, D. W. C. MacMillan, *Chem. Rev.* **2022**, *122*, 1485–1542.
[28] N. F. Nikitas, P. L. Gkizis, C. G. Kokotos, *Org. Biomol. Chem.* **2021**, *19*, 5237–5253.
[29] L. Capaldo, D. Ravelli, *Eur. J. Org. Chem.* **2017**, *2017*, 2056–2071.
[30] H. Cao, X. Tang, H. Tang, Y. Yuan, J. Wu, *Chem Catal.* **2021**, *1*, 523–598.
[31] Z. Ye, Y. M. Lin, L. Gong, *Eur. J. Org. Chem.* **2021**, *2021*, 5545–5556.
[32] G. Lei, M. Xu, R. Chang, I. Funes-Ardoiz, J. Ye, *J. Am. Chem. Soc.* **2021**, *143*, 11251–11261.
[33] L. Capaldo, T. Noël, D. Ravelli, *Chem Catal.* **2022**, DOI 10.1016/j.checat.2022.03.005.
[34] S. J. Blanksby, G. B. Ellison, *Acc. Chem. Res.* **2003**, *36*, 255–263.
[35] A. A. Isse, C. Y. Lin, M. L. Coote, A. Gennaro, *J. Phys. Chem. B* **2011**, *115*, 678–684.
[36] Y. Shen, Y. Gu, R. Martin, *J. Am. Chem. Soc.* **2018**, *140*, 12200–12209.
[37] H. Wang, H. Liu, M. Wang, M. Huang, X. Shi, T. Wang, X. Cong, J. Yan, J. Wu, *iScience* **2021**, *24*, 102693.
[38] C. Shu, A. Noble, V. K. Aggarwal, *Nature* **2020**, *586*, 714–719.
[39] C. Bottecchia, F. Lévesque, J. P. McMullen, Y. Ji, M. Reibarkh, F. Peng, L. Tan, G. Spencer, J. Nappi, D. Lehnherr, K. Narsimhan, M. K. Wismer, L. Chen, Y. Lin, S. M. Dalby, *Org. Process Res. Dev.* **2021**, DOI 10.1021/acs.oprd.1c00240.
[40] P. Xu, P. Y. Chen, H. C. Xu, *Angew. Chem. Int. Ed.* **2020**, *59*, 14275–14280; *Angew. Chem.* **2020**, *132*, 14381–14386.
[41] R. K. Quinn, Z. A. Könst, S. E. Michalak, Y. Schmidt, A. R. Szklarski, A. R. Flores, S. Nam, D. A. Horne, C. D. Vanderwal, E. J. Alexanian, *J. Am. Chem. Soc.* **2016**, *138*, 696–702.
[42] C. Y. Huang, J. Li, C. J. Li, *Nat. Commun.* **2021**, *12*, 1–9.
[43] H.-C. Li, G.-N. Li, K. Sun, X.-L. Chen, M.-X. Jiang, L.-B. Qu, B. Yu, *Org. Lett.* **2022**, *24*, 2431–2435.
[44] W. Liu, Q. Wu, M. Wang, Y. Huang, P. Hu, *Org. Lett.* **2021**, *23*, 8413–8418.
[45] Y. Abderrazak, A. Bhattacharyya, O. Reiser, *Angew. Chem. Int. Ed.* **2021**, *60*, 21100–21115.
[46] J. K. Kochi, *J. Am. Chem. Soc.* **1962**, *84*, 2121–2127.
[47] G. B. Shul'pin, M. M. Kats, *React. Kinet. Catal. Lett.* **1990**, *41*, 239–243.
[48] G. B. Shul'pin, A. N. Druzhinina, L. S. Shul'pina, *Pet. Chem.* **1993**, *33*, 321–325.
[49] K. Takaki, J. Yamamoto, Y. Matsushita, H. Morii, T. Shishido, K. Takehira, *Bull. Chem. Soc. Jpn.* **2003**, *76*, 393–398.
[50] K. Takaki, J. Yamamoto, K. Komeyama, T. Kawabata, K. Takehira, *Bull. Chem. Soc. Jpn.* **2004**, *77*, 2251–2255.
[51] A. J. Esswein, D. G. Nocera, *Chem. Rev.* **2007**, *107*, 4022–4047.
[52] T. S. Teets, D. G. Nocera, *Chem. Commun.* **2011**, *47*, 9268–9274.

[53] S. J. Hwang, B. L. Anderson, D. C. Powers, A. G. Maher, R. G. Hadt, D. G. Nocera, *Organometallics* **2015**, *34*, 4766–4774.
[54] S. J. Hwang, D. C. Powers, A. G. Maher, B. L. Anderson, R. G. Hadt, S. L. Zheng, Y. S. Chen, D. G. Nocera, *J. Am. Chem. Soc.* **2015**, *137*, 6472–6475.
[55] S. K. Kariofillis, A. G. Doyle, *Acc. Chem. Res.* **2021**, *54*, 988–1000.
[56] B. J. Shields, A. G. Doyle, *J. Am. Chem. Soc.* **2016**, *138*, 12719–12722.
[57] M. K. Nielsen, B. J. Shields, J. Liu, M. J. Williams, M. J. Zacuto, A. G. Doyle, *Angew. Chem. Int. Ed.* **2017**, *56*, 7191–7194; *Angew. Chem.* **2017**, *129*, 7297–7300.
[58] S. K. Kariofillis, B. J. Shields, M. A. Tekle-Smith, M. J. Zacuto, A. G. Doyle, *J. Am. Chem. Soc.* **2020**, *142*, 7683–7689.
[59] L. K. G. Ackerman, J. I. Martinez Alvarado, A. G. Doyle, *J. Am. Chem. Soc.* **2018**, *140*, 14059–14063.
[60] G. S. Lee, J. Won, S. Choi, M. H. Baik, S. H. Hong, *Angew. Chem. Int. Ed.* **2020**, *59*, 16933–16942; *Angew. Chem.* **2020**, *132*, 17081–17090.
[61] M. S. Santos, A. G. Corrêa, M. W. Paixão, B. König, *Adv. Synth. Catal.* **2020**, *362*, 2367–2372.
[62] H. P. Deng, X. Z. Fan, Z. H. Chen, Q. H. Xu, J. Wu, *J. Am. Chem. Soc.* **2017**, *139*, 13579–13584.
[63] L. Buglioni, F. Raymenants, A. Slattery, S. D. A. Zondag, T. Noël, *Chem. Rev.* **2022**, *122*, 2752–2906.
[64] D. Cambié, C. Bottecchia, N. J. W. Straathof, V. Hessel, T. Noël, *Chem. Rev.* **2016**, *116*, 10276–10341.
[65] S. Y. Go, G. S. Lee, S. H. Hong, *Org. Lett.* **2018**, *20*, 4691–4694.
[66] N. A. Till, R. T. Smith, D. W. C. MacMillan, *J. Am. Chem. Soc.* **2018**, *140*, 5701–5705.
[67] Y. Jin, Q. Zhang, L. Wang, X. Wang, C. Meng, C. Duan, *Green Chem.* **2021**, *23*, 6984–6989.
[68] Q. Zhang, S. Liu, J. Lei, Y. Zhang, C. Meng, C. Duan, Y. Jin, *Org. Lett.* **2022**, *24*, 1901–1906.
[69] Y. Jin, L. Wang, Q. Zhang, Y. Zhang, Q. Liao, C. Duan, *Green Chem.* **2021**, *23*, 9406–9411.
[70] Y. C. Kang, S. M. Treacy, T. Rovis, *ACS Catal.* **2021**, *11*, 7442–7449.
[71] Y. C. Kang, S. M. Treacy, T. Rovis, *Synlett* **2021**, *32*, 1767–1771.
[72] S. M. Treacy, T. Rovis, *J. Am. Chem. Soc.* **2021**, *143*, 2729–2735.
[73] R. A. Sheldon, J. K. Kochi, *J. Am. Chem. Soc.* **1968**, *90*, 6688–6698.
[74] A. Hu, J. J. Guo, H. Pan, H. Tang, Z. Gao, Z. Zuo, *J. Am. Chem. Soc.* **2018**, *140*, 1612–1616.
[75] A. Hu, J. J. Guo, H. Pan, Z. Zuo, *Science* **2018**, *361*, 668–672.
[76] Q. An, Z. Wang, Y. Chen, X. Wang, K. Zhang, H. Pan, W. Liu, Z. Zuo, *J. Am. Chem. Soc.* **2020**, *142*, 6216–6226.
[77] Q. Yang, Y. H. Wang, Y. Qiao, M. Gau, P. J. Carroll, P. J. Walsh, E. J. Schelter, *Science* **2021**, *372*, 847–852.
[78] J. Xu, H. Cai, J. Shen, C. Shen, J. Wu, P. Zhang, X. Liu, *J. Org. Chem.* **2021**, *86*, 17816–17832.
[79] M. Yamane, Y. Kanzaki, H. Mitsunuma, M. Kanai, *Org. Lett.* **2022**, *24*, 1486–1490.
[80] G. B. Panetti, Q. Yang, M. R. Gau, P. J. Carroll, P. J. Walsh, E. J. Schelter, *Chem Catal.* **2022**, *2*, 853–866.
[81] A. Pulcinella, D. Mazzarella, T. Noël, *Chem. Commun.* **2021**, *57*, 9956–9967.
[82] K. Ohkubo, A. Fujimoto, S. Fukuzumi, *Chem. Commun.* **2011**, *47*, 8515–8517.
[83] K. Ohkubo, K. Mizushima, S. Fukuzumi, *Res. Chem. Intermed.* **2013**, *39*, 205–220.
[84] Z. Luo, Z. H. Gao, Z. Y. Song, Y. F. Han, S. Ye, *Org. Biomol. Chem.* **2019**, *17*, 4212–4215.
[85] S. Rohe, A. O. Morris, T. McCallum, L. Barriault, *Angew. Chem. Int. Ed.* **2018**, *57*, 15664–15669; *Angew. Chem.* **2018**, *130*, 15890–15895.
[86] M. Zidan, A. O. Morris, T. McCallum, L. Barriault, *Eur. J. Org. Chem.* **2020**, *2020*, 1453–1458.
[87] H. P. Deng, Q. Zhou, J. Wu, *Angew. Chem. Int. Ed.* **2018**, *57*, 12661–12665; *Angew. Chem.* **2018**, *130*, 12843–12847.
[88] Z. Wang, X. Ji, T. Han, G. J. Deng, H. Huang, *Adv. Synth. Catal.* **2019**, *361*, 5643–5647.
[89] Z. Wang, Q. Liu, X. Ji, G. J. Deng, H. Huang, *ACS Catal.* **2020**, *10*, 154–159.
[90] X. Ji, Q. Liu, Z. Wang, P. Wang, G. J. Deng, H. Huang, *Green Chem.* **2020**, *22*, 8233–8237.
[91] C. Wang, H. Shi, G. J. Deng, H. Huang, *Org. Biomol. Chem.* **2021**, *19*, 9177–9181.
[92] Z. Sun, H. Huang, Q. Wang, G. J. Deng, *Adv. Synth. Catal.* **2022**, *364*, 453–458.
[93] T. Kawasaki, N. Ishida, M. Murakami, *J. Am. Chem. Soc.* **2020**, *142*, 3366–3370.
[94] N. Ishida, M. Son, T. Kawasaki, M. Ito, M. Murakami, *Synlett* **2021**, *32*, 2067–2070.
[95] T. Kawasaki, N. Ishida, M. Murakami, *Angew. Chem. Int. Ed.* **2020**, *59*, 18267–18271; *Angew. Chem.* **2020**, *132*, 18424–18428.
[96] T. Kawasaki, T. Tosaki, N. Ishida, M. Murakami, *Org. Lett.* **2021**, *23*, 7683–7687.
[97] O. M. Griffiths, H. A. Esteves, Y. Chen, K. Sowa, O. S. May, P. Morse, D. C. Blakemore, S. V. Ley, *J. Org. Chem.* **2021**, *86*, 13559–13571.
[98] X. Shu, L. Huan, Q. Huang, H. Huo, *J. Am. Chem. Soc.* **2020**, *142*, 19058–19064.
[99] W. Zhang, X. Shu, L. Huan, B. Cheng, H. Huo, *Org. Biomol. Chem.* **2021**, *19*, 9407–9409.
[100] J. Xu, Z. Li, Y. Xu, X. Shu, H. Huo, *ACS Catal.* **2021**, *11*, 13567–13574.
[101] L. Huan, X. Shu, W. Zu, D. Zhong, H. Huo, *Nat. Commun.* **2021**, *12*, DOI 10.1038/s41467-021-23887–2.
[102] C. L. Cao, G. X. Zhang, F. Xue, H. P. Deng, *Org. Chem. Front.* **2022**, *9*, 959–965.
[103] S. K. Kariofillis, S. Jiang, A. M. Żurański, S. S. Gandhi, J. I. Martinez Alvarado, A. G. Doyle, *J. Am. Chem. Soc.* **2022**, *144*, 1045–1055.
[104] P. Jia, Q. Li, W. C. Poh, H. Jiang, H. Liu, H. Deng, J. Wu, *Chem* **2020**, *6*, 1766–1776.
[105] F. Strieth-Kalthoff, M. J. James, M. Teders, L. Pitzer, F. Glorius, *Chem. Soc. Rev.* **2018**, *47*, 7190–7202.
[106] D. R. Heitz, J. C. Tellis, G. A. Molander, *J. Am. Chem. Soc.* **2016**, *138*, 12715–12718.
[107] A. Dewanji, P. E. Krach, M. Rueping, *Angew. Chem. Int. Ed.* **2019**, *58*, 3566–3570; *Angew. Chem.* **2019**, *131*, 3604–3608.
[108] S. Das, K. Murugesan, G. J. Villegas Rodríguez, J. Kaur, J. P. Barham, A. Savateev, M. Antonietti, B. König, *ACS Catal.* **2021**, *11*, 1593–1603.
[109] L. Huang, M. Rueping, *Angew. Chem. Int. Ed.* **2018**, *57*, 10333–10337; *Angew. Chem.* **2018**, *130*, 10490–10494.
[110] Z. Sun, N. Kumagai, M. Shibasaki, *Org. Lett.* **2017**, *19*, 3727–3730.
[111] X. Cheng, H. Lu, Z. Lu, *Nat. Commun.* **2019**, *10*, 1–7.
[112] X. Cheng, T. Li, Y. Liu, Z. Lu, *ACS Catal.* **2021**, *11*, 11059–11065.
[113] N. Ishida, Y. Masuda, N. Ishikawa, M. Murakami, *Asian J. Org. Chem.* **2017**, *6*, 669–672.
[114] M. I. Gonzalez, D. Gygi, Y. Qin, Q. Zhu, E. J. Johnson, Y. S. Chen, D. G. Nocera, *J. Am. Chem. Soc.* **2022**, *144*, 1464–1472.
[115] G. A. Russell, *J. Am. Chem. Soc.* **1957**, *79*, 2977–2978.
[116] G. A. Russell, *J. Am. Chem. Soc.* **1958**, *80*, 4987–4996.
[117] C. Walling, M. F. Mayahi, *J. Am. Chem. Soc.* **1959**, *81*, 1485–1489.
[118] S. Förgeteg, T. Bérces, *J. Photochem. Photobiol. A* **1993**, *73*, 187–195.
[119] R. Breslow, M. Brandi, J. Hunger, N. Turro, K. Cassidy, K. Krogh-Jespersen, J. D. Westbrook, *J. Am. Chem. Soc.* **1987**, *109*, 7204–7206.
[120] S. Escoubet, S. Gastaldi, N. Vanthuyne, G. Gil, D. Siri, M. P. Bertrand, *J. Org. Chem.* **2006**, *71*, 7288–7292.
[121] T. Noël, E. Zysman-Colman, *Chem Catal.* **2022**, *2*, 468–476.

Manuscript received: April 6, 2022
Revised manuscript received: May 11, 2022
Accepted manuscript online: May 12, 2022

REVIEW

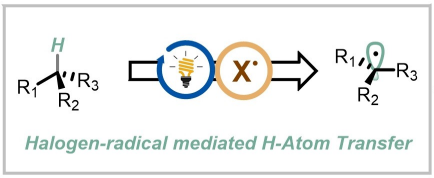

*S. Bonciolini, Prof. Dr. T. Noël, Dr. L. Capaldo**

Photocatalysis is a method of choice for the generation of reactive intermediates under mild conditions. This Review collects the recent examples exploiting this manifold to generate highly aggressive halogen radicals to activate C(sp^3)–H bonds via Hydrogen Atom Transfer (HAT) for synthetic purposes. Available strategies to influence site-selectivity of the hydrogen atom transfer step have also been discussed.